26

DAVID BLOOM

TECTONICS, VOL. 7, NO. 6, PAGES 1141-1166, DECEMBER 1988

TATLA LAKE METAMORPHIC COMPLEX: AN EOCENE METAMORPHIC CORE COMPLEX ON THE SOUTHWESTERN EDGE OF THE INTERMONTANE BELT OF BRITISH COLUMBIA

R. M. Friedman and Richard Lee Armstrong

Department of Geological Sciences, University of British Columbia, Vancouver, Canada

Abstract. The Tatla Lake Metamorphic Complex (TLMC), which lies on the southwest side of the Intermontane Belt (IMB) in British Columbia, has characteristics typical of a metamorphic core complex: anticlinorial amphibolite-grade gneissic and migmatitic core underlying a 1- to 2.5+-km-thick zone of mylonite and ductilely sheared metamorphic rocks which is in fault contact beneath an upper plate of low-metamorphic-grade cover rocks of the IMB. Ductile shearing in the TLMC involved tonalitic to granodioritic orthogneiss and structurally overlying amphibolite-grade metasedimentary rocks and greenschist-grade chlorite-actinolite-albite schist. Structures observed throughout the ductilely sheared rocks include a gently dipping mylonitic foliation (Ss), containing a mineral lineation (Ls) which trends toward 280°(100°) ± 20°. Minor folds of variable trend (Fs), almost exclusively confined to metasedimentary rocks, are interpreted as synductile shear. Vergence of these folds defines a movement sense and direction of top toward 290° ± 20°. Kinematic indicators from rocks not deformed by synductile shear folds indicate a tops-to-the-west sense of shear, while those within metasedimentary rocks (deformed by Fs folds) yield conflicting results, with a tops-to-the-west sense predominating. Calculated a directions from Fs folds which deform Ls lineations indicate nearly horizontal Ds movement, subparallel to 290°-110°. The entire metamorphic core of the TLMC has been deformed by upright, west to west-northwest trending, shallowly plunging map-scale folds (F3). The steeply dipping, northwest trending Yalakom fault cuts all units and forms the southwestern margin of the TLMC. U-Pb zircon geochronology has documented the existence of Cretaceous (107-79 Ma, in the core) and Eocene 55-47 Ma, in the mylonitic zone) deformation and metamorphism in the TLMC. K-Ar dates for biotite and hornblende of 53.4-45.6 Ma record the uplift and cooling of the TLMC. During early and middle Eocene time (55-47 Ma) metamorphic rocks of the TLMC were carried to higher crustal levels along the footwall of the TLMC normal ductile shear zone. Final uplift and development of F3 folds (post-47 Ma) are possibly related to dextral motion along the Yalakom fault. The TLMC has structural style and timing of deformation similar to other metamorphic core complexes in southeastern British Columbia. Local and regional evidence is consistent with the formation of the TLMC in a regional extensional setting within a vigorous magmatic arc. Similar interlayered gneisses with near-horizontal layering and foliation may underlie the entire southern IMB.

Paper number 88TC03254.
0278-7407/88/88TC-03254$10.00

INTRODUCTION

This paper reports the results of a study of the best exposed portions of a discontinuous, northwest trending area of unnamed gneissic rocks (Figure 1) shown on 1:250,000 scale maps by Tipper [1969a, map unit A; 1969b, map unit 3]. A nongenetic name proposed and used herein for these gneissic rocks is the Tatla Lake Metamorphic

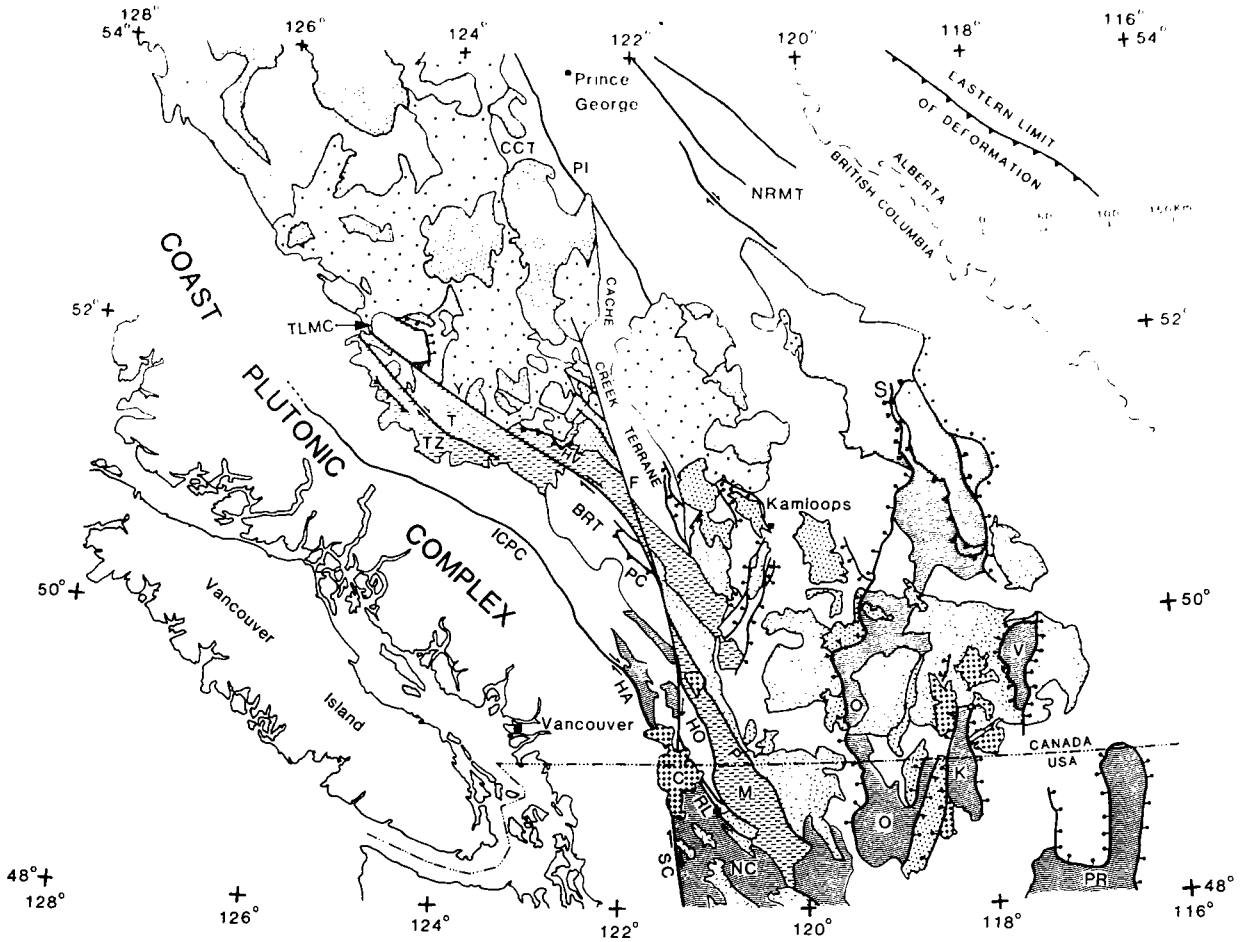

Fig. 1. Geological map of southern British Columbia and adjacent areas east of the Coast Plutonic Complex. Eocene faults are highlighted. Normal faults, balls on upper plate; thrust faults: teeth on upper plate. Modified from Tipper et al. [1981], Gabites [1985], Carr et al. [1987], Parrish et al. [1988], and Wheeler and McFeely [1987]. BRT, Bridge River Terrane; CCT, Cache Creek Terrane; F, Fraser fault; HA, Harrison Lake fault; HO, Hozameen fault; HV, Hungry Valley fault; ICPC, Intra Coast Plutonic Complex fault; K, Kettle Complex; M, Methow Basin; NC, North Cascades; NRMT, Northern Rocky Mountain Trench fault System, southern splays; O, Okanagan Complex in British Columbia, Okanogan Complex in Washington; PC, Phair Creek fault; P, Pasaytan fault; PI, Pinchi fault; PR, Priest River Complex; RL, Ross Lake Shear Zone; S, Shuswap Complex; SC, Straight Creek fault; T, Tyaughton Basin; TZ, Tchaikazan fault V, Valhalla Complex; Y, Yalakom fault.

Complex (TLMC). This study includes bedrock mapping, structural analysis, U-Pb and K-Ar geochronometry, petrology, and a regional tectonic synthesis. The TLMC was chosen for study because detailed lithologic and structural information was lacking in this area, which had formerly only been mapped on a reconnaissance basis [Dawson, 1876; Dolmage, 1926; Tipper, 1969a,b], and it provided a unique opportunity to sample and study Intermontane Belt (IMB) rocks from midcrustal depths. This is the only area of higher-grade metamorphic rocks between the large exposures of midcrustal high-grade rocks of the Coast and Omineca belts which lie to the west and east of the IMB. Information about structural style and timing(s) of deformation and magmatism in the TLMC can be applied to problems such as the relationship between the TLMC and low-grade cover rocks of the IMB and timing of motion along the Yalakom fault.

GENERAL GEOLOGY

The TLMC has the characteristics of a metamorphic core complex [Coney, 1980; Armstrong, 1982]. The study area can be divided into three

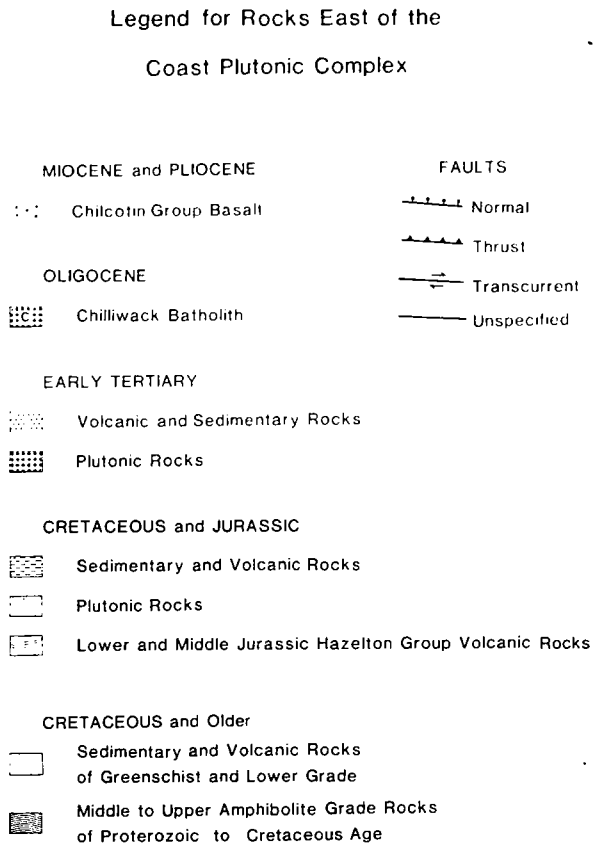

Fig. 1. (continued)

structural levels (Figure 2a). In ascending structural order these are (1) middle to upper amphibolite-grade gneissic and migmatitic core, (2) gently dipping amphibolite and greenschist-grade mylonitic schist and gneiss (ductilely sheared assemblage), and (3) low metamorphic grade cover rocks preserving primary fabrics. Faults separate rocks of the metamorphic core (TLMC, structural levels 1 and 2, lower plate) from IMB cover rocks (upper plate) to the south and east (Figure 2a). Upper plate rocks of the IMB adjacent to the TLMC include Jurassic (?) volcanic breccias and flows (possibly correlative with the upper part of the Hazelton volcanics to the north), Jurassic (?) granitic intrusives, Cretaceous to early Tertiary volcanic rocks, and the Miocene Chilcotin Group basalts (Figure 1) [Tipper, 1969a,b; Bevier, 1983].

The southwestern margin of the TLMC is the steeply dipping Yalakom fault, which cuts both lower and upper plates. This fault has commonly been interpreted as a dextral transcurrent system [Tipper, 1969a; Kleinspehn, 1985]. Tipper [1969a] has suggested about 150 km of dextral offset along the segment of the Yalakom adjacent to the TLMC based on a correlation of Jurassic volcanic rocks on both sides of the fault. A truncated western continuation of the TLMC has not yet been recognized southwest of the Yalakom fault. The fault has only been followed to about 52° N, at the north end of the TLMC, where it abruptly disappears into the Coast Plutonic Complex.

The rocks directly to the southwest of the Yalakom fault near the TLMC include a Late Triassic marine volcanic arc assemblage, Jura-Cretaceous clastic sediments of the Tyaughton trough, and Jurassic to Eocene granitic intrusions of the Coast Plutonic Complex [Tipper, 1969a; Kleinspehn, 1985; Rusmore, 1985]. Stratified rocks as young as Hauterivian in age have been deformed by dominantly northeasterly verging folds and thrusts [Tipper, 1969a].

GNEISSIC CORE

Gneiss

The core of the TLMC is made up of gneiss and migmatitic gneiss. Migmatitic gneiss occupies the deepest structural levels and is composed of about 60% biotite-hornblende gneiss and 40% migmatitic veins of tonalitic to granodioritic composition, interlayered on the centimeter to meter scale. Structurally upward in the gneiss the proportion of migmatitic veins decreases to less than about 10%; the transition is gradational rather than abrupt.

The gneiss is medium to coarse grained with granoblastic elongate texture [Spry, 1969, p. 263] and consists of plagioclase ($>An_{30}$) + biotite + quartz + hornblende ± garnet. Overall, the relative proportions of phases and homogenous nature of the gneiss are consistent with a plutonic parentage. There are however, small areas of relatively biotite and garnet rich gneiss that could have been derived from a sedimentary protolith.

There is commonly one foliation present in the gneiss (S1c; see Table 1 for explanation of structural element terminology, Figure 2b for generalized structural data, Figure 3 for structural domains and Figure 4 for stereoplots of structural data), defined by a biotite schistosity as well as the overall gneissosity of the rock. A weak to moderate west-northwest to (rarely) west-southwest trending mineral elongation lineation (L2c) is defined by hornblende, plagioclase, and quartz.

Two superposed generations of mesoscopic folds have been recognized in the gneiss and migmatitic gneiss, both of which are west-northwest to (rarely) west-southwest trending, shallowly plunging and fold S1c (Figures 2a, 2b). The earlier of the two, F2c is tight to isoclinal and parallel to the L2c lineation (Figures 4d and 4e). These folds have not been recognized at the map scale. F3 folds are upright, occur on all scales, and involve the entire metamorphic core of the TLMC. These

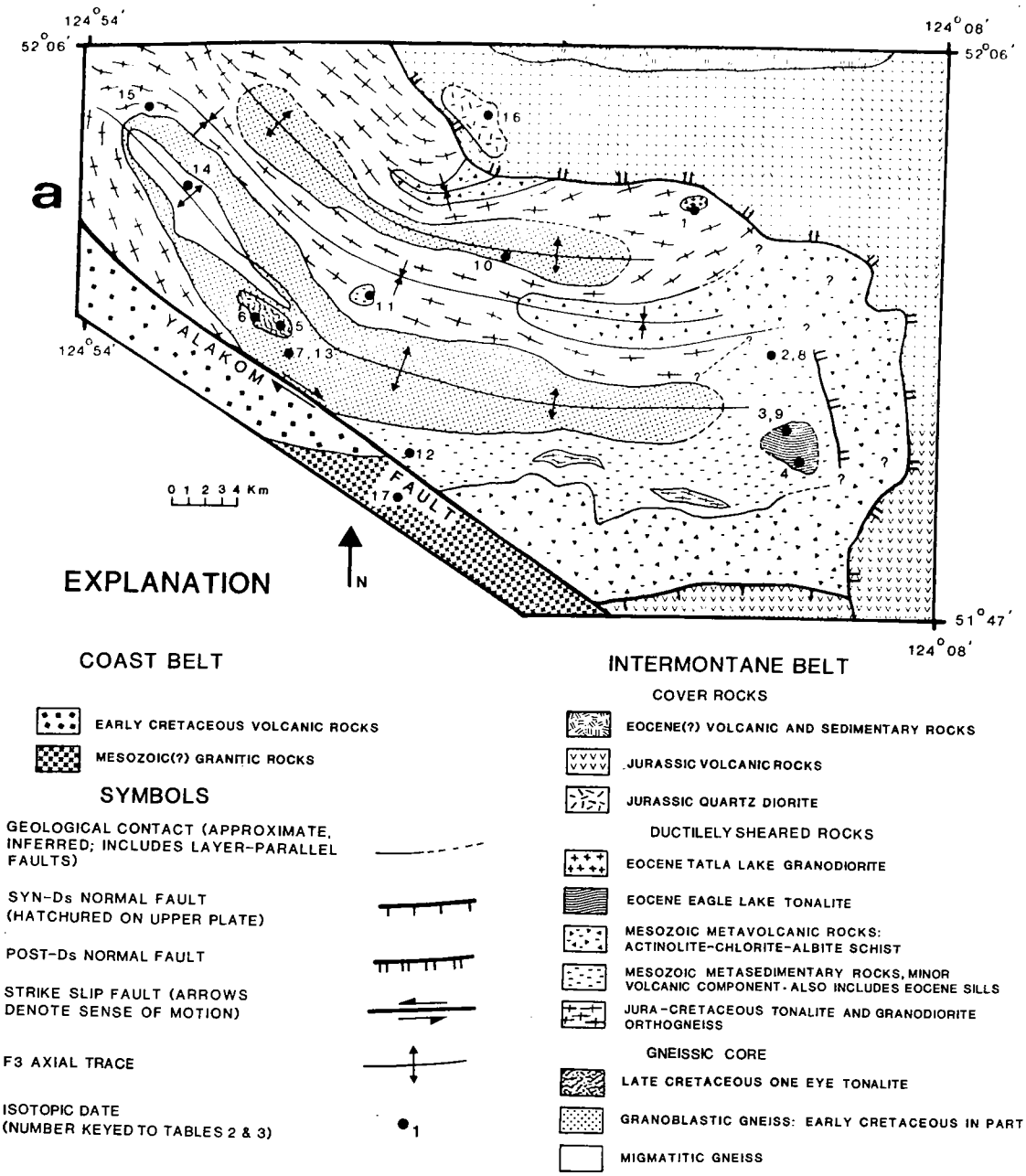

Fig. 2. Generalized maps of the Tatla Lake Metamorphic Complex. (a) Geological map; approximate contacts are located to within ± 500 m. (b) Simplified structural map; see Table 1 for explanation of structural element terminology.

structures are best developed in the gneissic core of the TLMC, decreasing in intensity at higher structural levels and in an east-southeasterly direction across the study area (Figures 4f and 4g). The open to normal geometry and lack of fabric associated with F3 folds suggest that they formed at low metamorphic grade. On the outcrop scale, the superposition of F3 upon F2c fold sets has resulted in type 3 fold interference patterns [Ramsay, 1967]. This fold set deforms both the S1c foliation and F2c axial surfaces (Figures 4d and 4e).

Plagioclase ($>An_{30}$) and hornblende in the gneiss indicate that metamorphic recrystallization took place under amphibolite facies conditions [Wenk and Keller, 1969; Turner and Verhoogen,

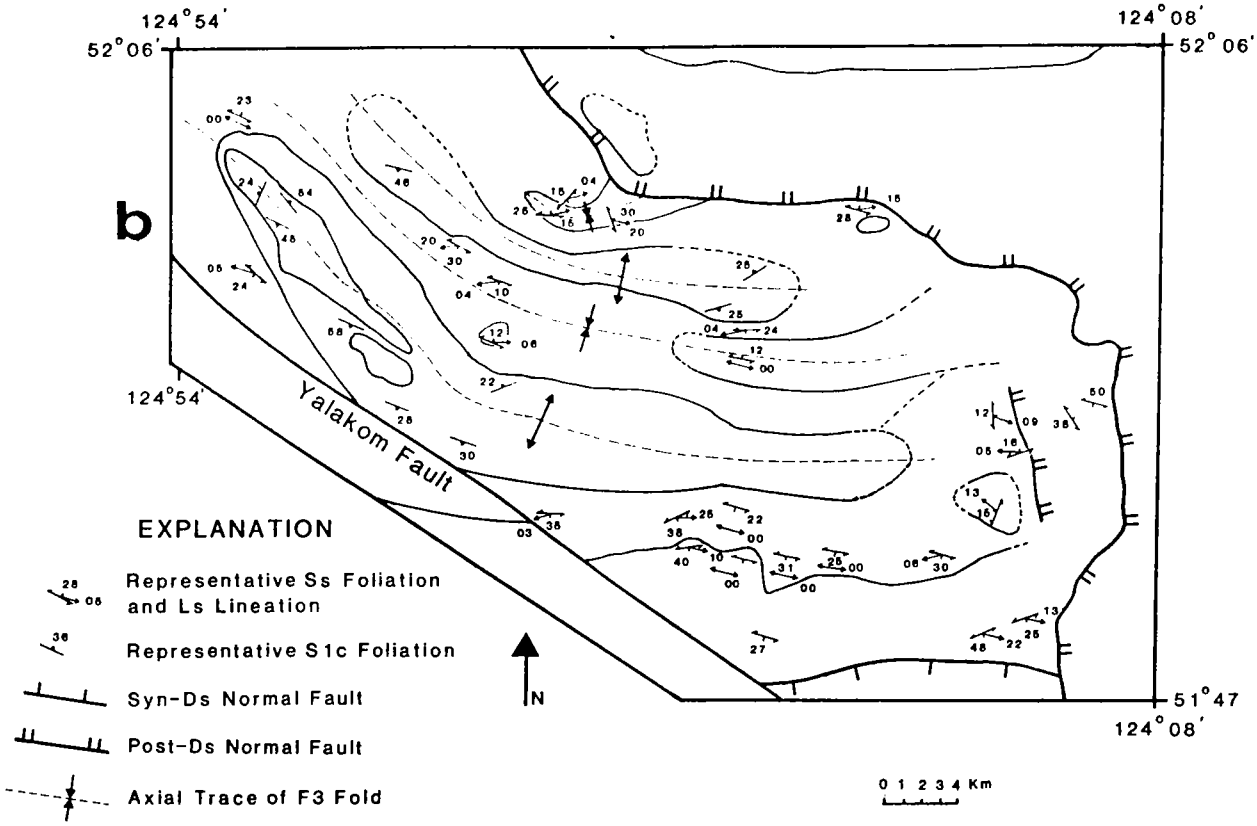

Fig. 2. (continued)

1960]. The presence of small post-F2c pegmatitic clots with graphic texture, consisting of plagioclase + quartz + alkali feldspar + biotite + muscovite + garnet or plagioclase + hornblende + biotite + quartz, indicates that incipient partial melting occurred, and this suggests that upper amphibolite facies conditions were attained at the peak of metamorphism [Winkler, 1976, pp. 83–84].

One Eye Tonalite

The One Eye tonalite intrudes the gneissic core of the TLMC (Figure 2a). It consists of medium- to coarse-grained plagioclase + biotite + hornblende + quartz. Along the margin of this intrusion a schistosity, parallel to S1c in the enclosing gneiss, has been observed. The intensity of this fabric diminishes toward the interior, becoming indistinct in the core. The One Eye tonalite is less strained than the surrounding gneiss and is interpreted as a late synkinematic body.

DUCTILELY SHEARED ASSEMBLAGE

General Discussion

The upper part of the TLMC is a lithologically heterogeneous and variably metamorphosed 1- to 2.5+-km-thick ductile shear zone. Most of this zone is made up of mylonitic orthogneiss and structurally overlying metasedimentary and metavolcanic rocks (Figure 2a). The Eagle Lake biotite tonalite (Figure 2a) and sills of intermediate to felsic composition intrude and are deformed in the shear zone. Intrusive, undeformed rocks which postdate activity along the shear zone include the Tatla Lake granodioritic stock (Figure 2a) and MacIntyre Island rhyolitic dykes. In the northwestern part of the study area the ductilely sheared rocks had a plutonic protolith, and in the southeastern part they had a largely stratified protolith. The involvement of structurally deeper plutonic rocks toward the northwest suggests that the shear zone cuts downsection toward the northwest.

The structural elements (see Table 1) common throughout the ductilely sheared assemblage (DSA) include a well-developed, shallowly plunging stretching lineation (Ls), defined by quartz, amphibole, and feldspar, which trends toward 280°(100°) ± 20° and a gently dipping mylonitic foliation (Ss), which parallels transposed layering in stratified lithologies and contains Ls (Figures 5a–5f). Tight to isoclinal mesoscopic folds (Fs, Figure 5g) of variable trend are almost exclusively confined to metasedimentary rocks of the ductile shear zone

TABLE 1. Terminology for Structural Elements in the TLMC

Term	Definition
Gneissic Core[a]	
S1c	Schistosity (defined by biotite) and gneissosity in the gneissic core.
F2c	Dominantly northwest trending, shallowly plunging, tight to isoclinal folds which deform S1c; not recognized at map scale.
S2c	Rarely observed axial plane cleavage associated with minor F2c folds.
L2c	Northwest trending mineral lineation defined by hornblende, plagioclase and quartz and associated with F2c structures.
Ductilely Sheared Rocks[b]	
Ss	Pervasive shallowly dipping mylonitic foliation defined by mica and ribbon quartz.
Ls	Mineral elongation (stretching) lineation defined by quartz, feldspar and amphibole trending toward 280° ± 20°.
Fs	Tight to isoclinal, shallowly plunging, variably trending mesoscopic folds
S2s	Localized axial plane crenulation cleavage associated with Fs folds; restricted to metasedimentary rocks and most well developed in metapelitic lithologies
Entire Metamorphic Complex	
F3	Open to normal east-west to northwest-southeast trending map scale folds which define the map pattern in the metamorphic core of the TLMC. Mesoscopic F3 folds are common in the gneissic core.

[a] Lower case 'c' denotes structural element observed exclusively in the gneissic core, dated at least in part as Cretaceous.

[b] Lower case 's' refers to structures observed throughout the ductilely sheared unit and at one locality structurally high in the gneissic core. The 's' structures have been dated as Eocene.

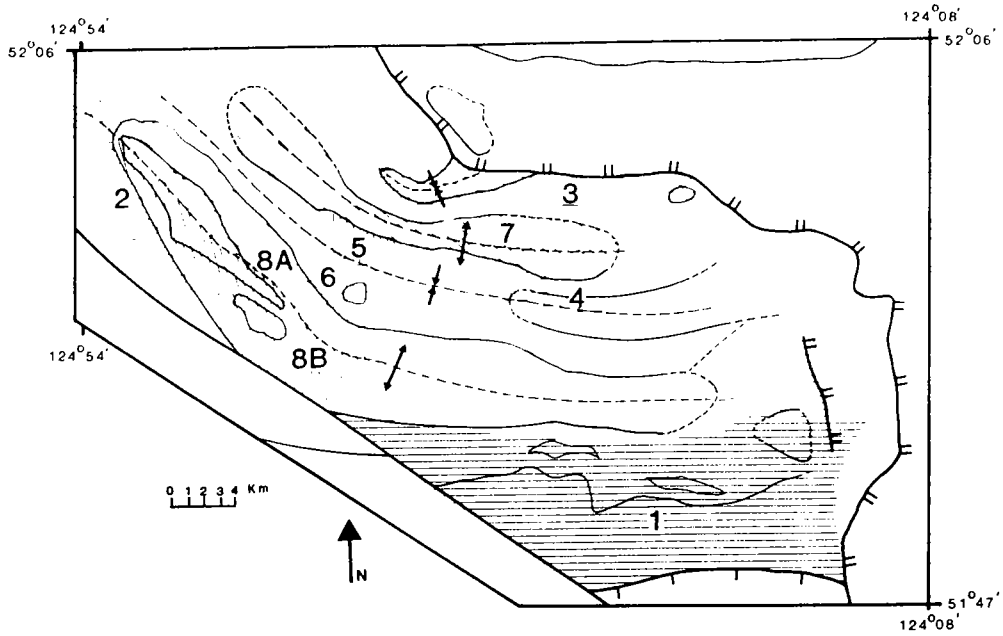

Fig. 3. Map showing the location and bounds of structural subareas in the TLMC.

and are interpreted to have developed during shear zone movement (discussed below).

Fold vergence defines a movement sense and direction of 290° ± 20° (Figure 5g) [Hansen, 1971]. A tops-to-the-west sense of shear was furthermore deduced for ductilely sheared rocks not involved in Fs folds, based on pressure shadows around asymmetric porphyroclasts/porphyroblasts, shear bands, S-C fabrics, microfaulted porphyroclasts, mica fish, and shape fabric in annealed ribbon quartz grains [Simpson and Schmid, 1983; Lister and Snoke, 1984] (Figure 6). Study of similar microstructures in metasedimentary rocks deformed by Fs folds has yielded conflicting results, with tops-to-the-west predominant.

The DSA has been deformed by map-scale F3

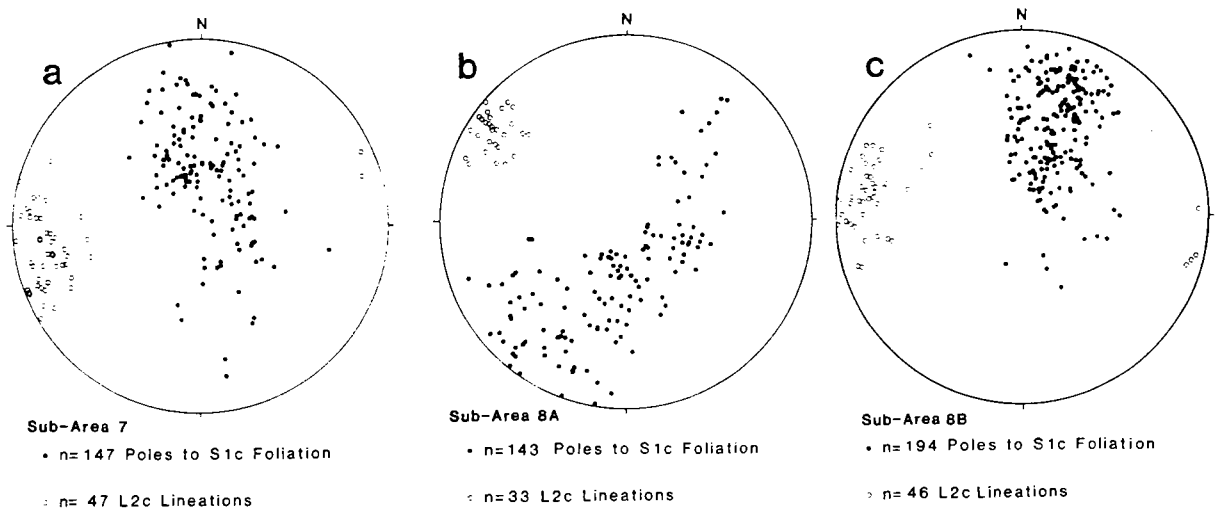

Fig. 4. Structural data from the TLMC plotted by structural subarea on lower hemisphere projections of equal-area stereonets. Data from the gneissic core. (a)-(c) Poles to S1c foliation; trend, plunge of L2c lineation, (d) and (e) Poles to F2c axial surfaces; trend, plunge F2c fold axes, (f) and (g) Poles to F3 axial surfaces; trend, plunge F3 fold axes.

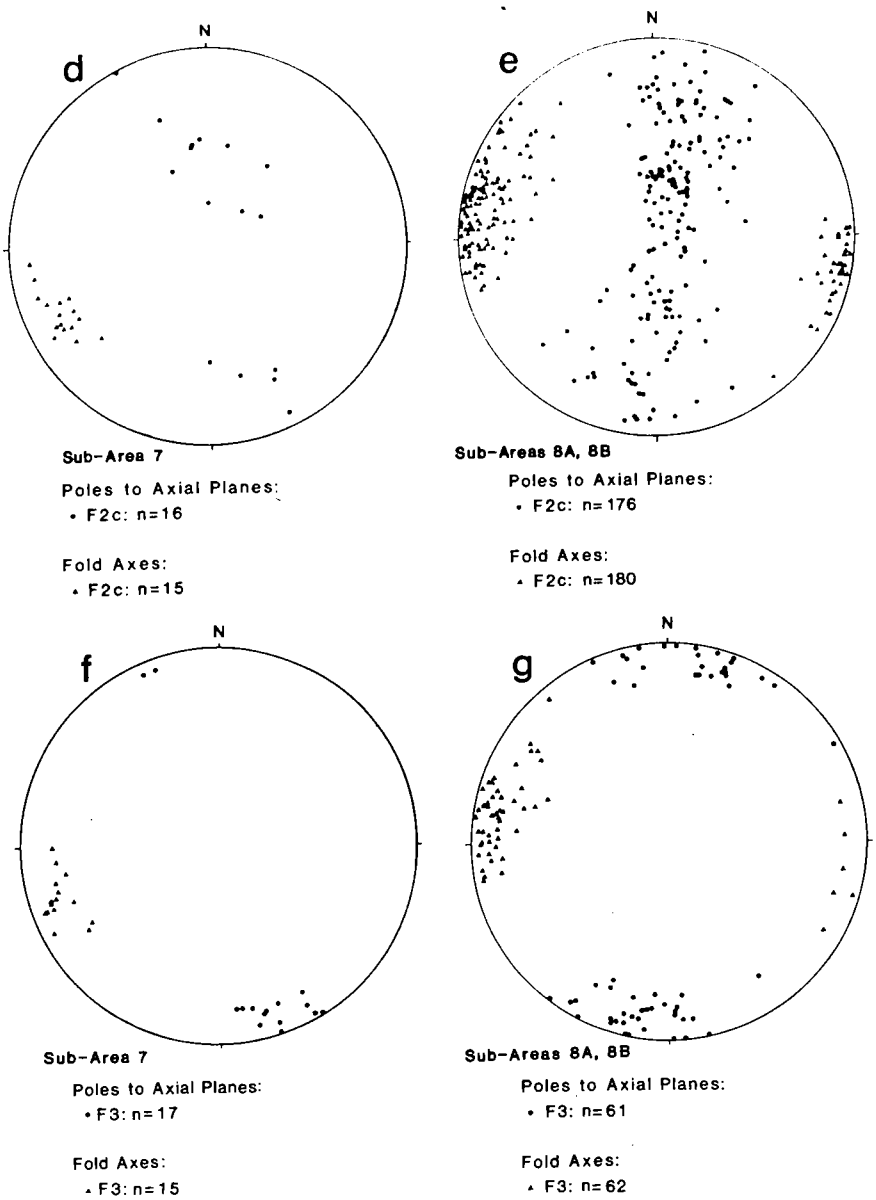

Fig. 4. (continued)

folds (Figures 2a, 2b, 4f and 4g). Outcrop scale F3 folds in these rocks are rare, unlike within the gneissic core. Outcrop is quite rare on north dipping limbs of F3 structures, rendering detailed structural geometries difficult to determine. The intensity of F3 folds decreases in an east-southeasterly direction across the study area.

Mylonitic Orthogneiss

Most of the DSA in the northern part of the map area and minor exposures in the southern part are mylonitic orthogneiss (Figure 2a). These rocks occur as lenticular or sheetlike bodies of medium- to coarse-grained, strongly foliated and lineated tonalitic to granodioritic orthogneiss. Ribbon quartz grains reach 3 cm in length and together with biotite ± muscovite define the Ss schistosity (Figure 6). The mylonitic orthogneiss unit is considered composite, based on its variable composition and age (Late Jurassic through Late Cretaceous U-Pb zircon dates [Friedman, 1988]).

The contact between mylonitic orthogneiss and structurally underlying rocks of the gneissic core

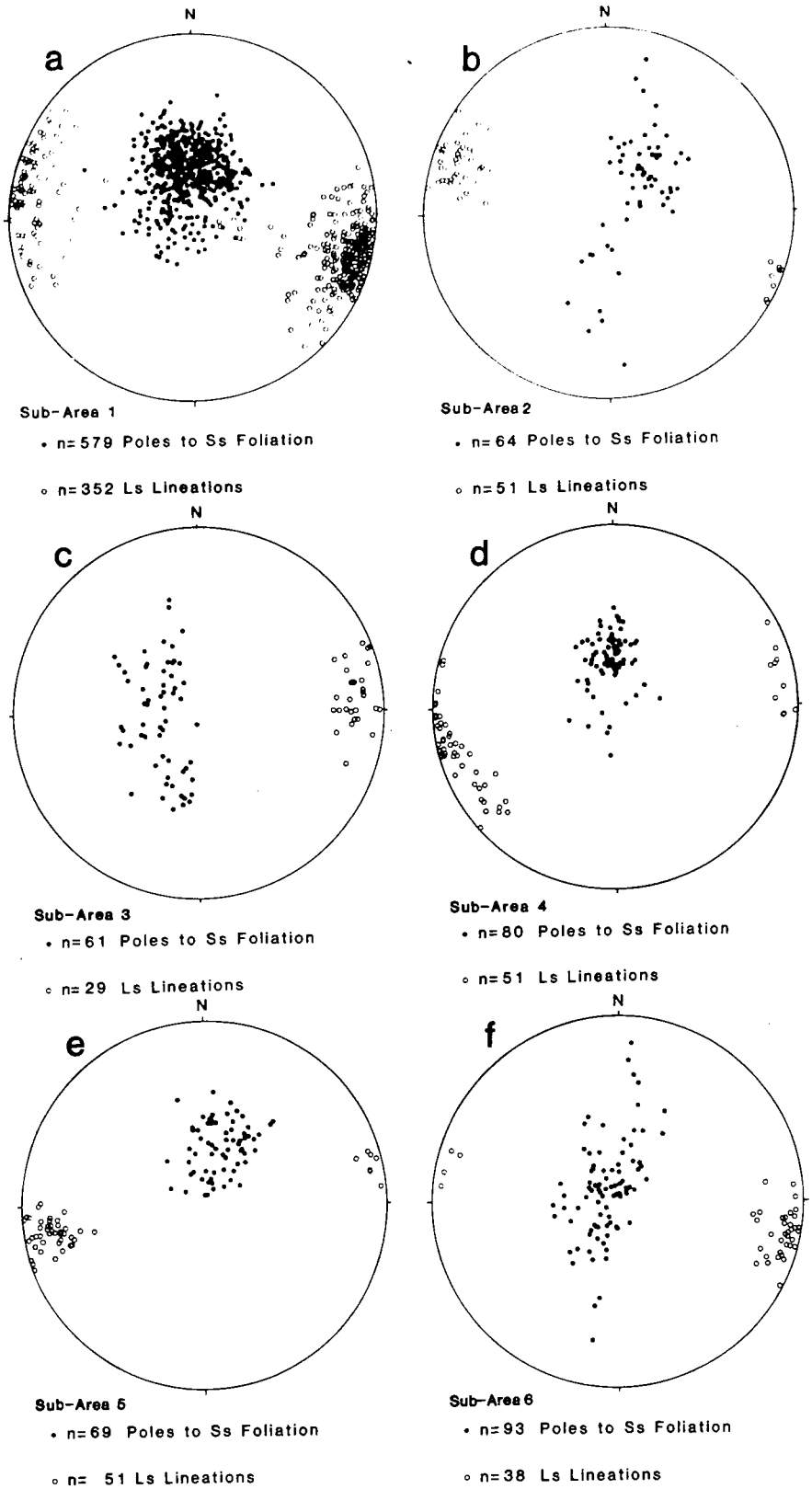

Fig. 5. Data from the DSA. (a)–(f) Poles to Ss foliation; trend, plunge of Ls lineation, (g) Poles to Fs axial surfaces; trend, plunge Fs fold axes. Arrows show sense of vergence for Fs folds.

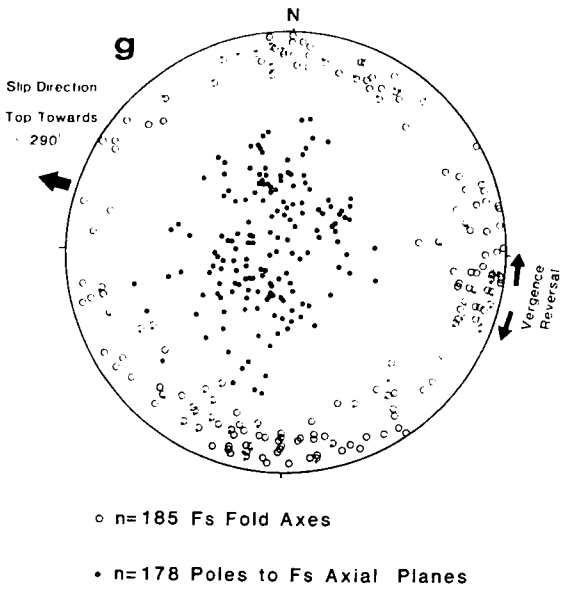

Fig. 5. (continued)

was not observed, but the covered zone between the two contrasting rock types is narrow, implying an abrupt change. The upper contact between orthogneiss and dominantly metasedimentary rocks is believed to be a ductile ± brittle fault, but field evidence is permissive rather than persuasive. Interlayering of lenticular orthogneiss with metasedimentary rocks has been observed at several localities.

Metasedimentary Rocks

An east-west trending belt of metasedimentary and subordinate metavolcanic rock outcrops in the southern part of the map area (Figure 2a). Their composition varies along strike, although quartzofeldspathic schist predominates. Pelitic schist occurs in the west central section of the outcrop belt. Rocks inferred to be metavolcanic in origin on the basis of composition occur throughout as hornblende + plagioclase ± quartz ± garnet-bearing and felsic layers 10 cm to 1 m thick and make up an estimated 10–15% of the section. TLMC metasedimentary rocks are lithologically correlated with sedimentary pods of varying dimensions occuring in Lower and Middle Jurassic volcanic rocks located to the east and northwest of the study area, on both sides of the Yalakom fault (Figure 1) [Tipper, 1969a,b; Baer, 1973].

Ls and Ss are well developed in the metasedimentary rocks. In addition, the metasedimentary rocks have been deformed by minor folds (Fs) that are almost exclusive to these rocks, probably due to the millimeter- to meter-scale compositional contrasts (producing ductility contrasts) not present in the more homogenous mylonitic orthogneiss and metavolcanic rocks.

Various lines of evidence indicate that Fs folds were progressivly developing while the TLMC shear zone was active. These folds are confined to the shear zone, yet do not deform the zone as a whole (Figure 2a). Axial surfaces dip shallowly and are subparallel to the shear zone boundaries (Figure 5g). Fs folds deform early mylonitic foliation and are truncated by subsequent mylonitic foliation, a feature common to folds developed in shear zones [Bell 1978; Bell and Hammond, 1984]. Fold axis trends are variable; a plot of all Fs fold axes (Figure 5g) defines a horizontal girdle. Within a single outcrop the trends of Fs fold hinges vary up to 70°, and up to 40° variations in fold axis orientation have been measured for single folds.

The tightest Fs folds (isoclinal) have axes which trend at small angles to the bulk stretching lineation direction (290°(110°) for the metasedimentary rocks), while folds with axes oblique to the stretching lineation direction (north-south trending) are more open (dihedral angles of 30°–70°; Figure 5g). The former were presumably developed early in the history of the shear zone, oblique to the stretching direction, and during progressive shear were reoriented into parallelism with it. The latter folds, which are common in the TLMC, may have formed late in the history of the shear zone. Folds of the latter geometry are reported to be rare in other ductile shear zones [Bell and Hammond, 1984].

As already mentioned, Fs fold vergence indicates a tops-to-the-west sense of shear [Christie, 1963; Hansen, 1971]. Fold vergence is a reliable kinematic indicator in shear zones where synshear fold axes are oblique to the bulk stretching lineation direction [Bell and Hammond, 1984], as is the case for the TLMC. In addition, a directions calculated for individual Fs folds which deform Ls lineations occur near the local Ls maxima (subarea 1; Figure 5a); they indicate a near-horizontal Ds movement direction, subparallel to 290°–110°.

Variable textural relationships of porphyroblasts in pelitic schist indicate that metamorphic recrystallization accompanied ductile deformation and continued until late to possibly post-Ds time. During a relatively early stage of porphyroblast growth, considered pre- to syn-Ds in timing, the composite mineral assemblage biotite + muscovite + quartz + garnet ± chloritoid ± staurolite ± kyanite crystallized. Mica (commonly isoclinally folded), which defines Ss schistosity, rolled garnet and pulled-apart staurolite characterize this early assemblage. (Figure 7a). Texturally early kyanite has only been recognized at one locality in the main belt of pelitic schist. A metamorphic peak of

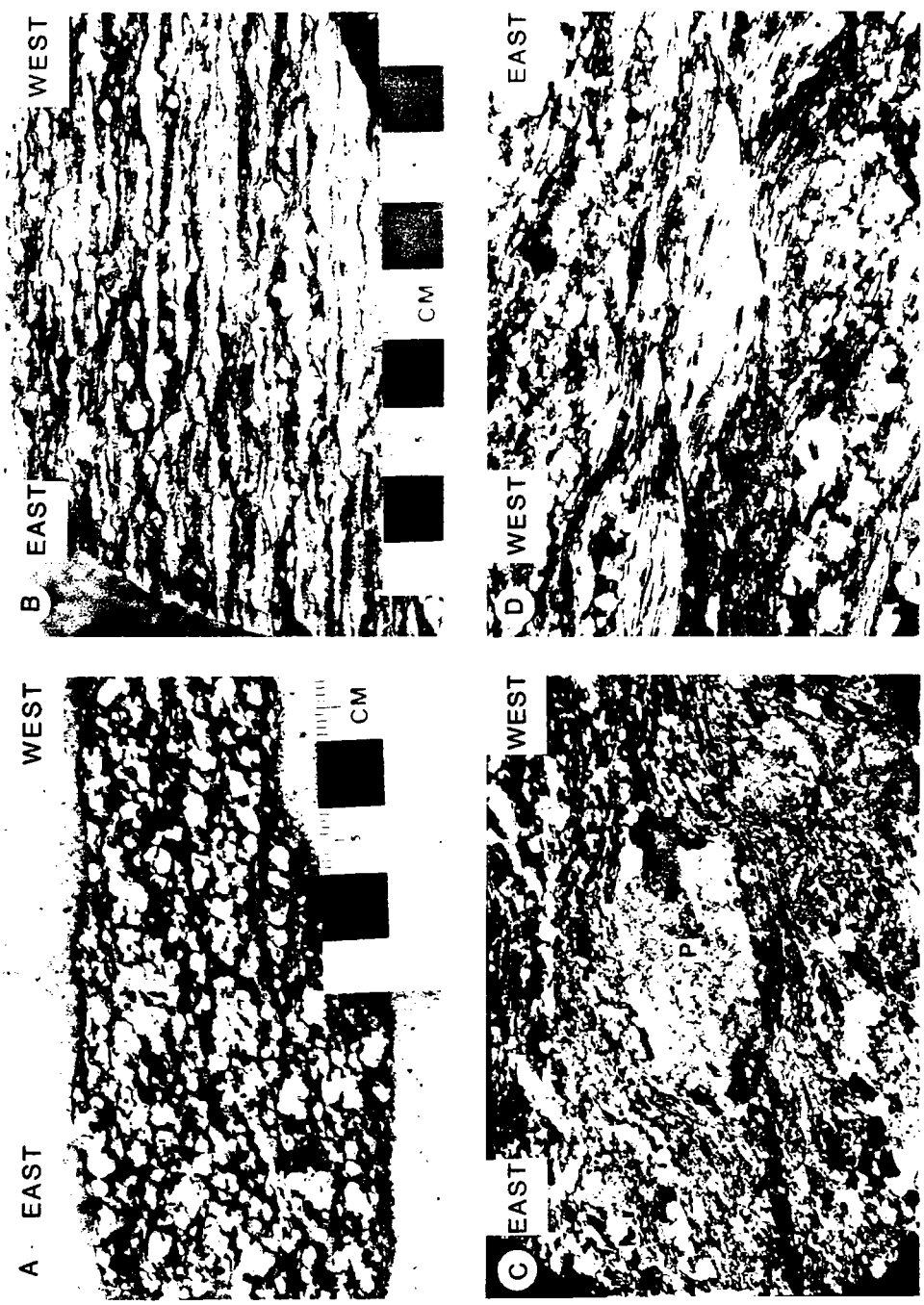

Fig. 6. Asymmetric textures in DSA rocks. Slabs and sections are cut parallel to Ls and perpendicular to Ss (X–Z section). Textures indicate a tops-to-the-west sense of shear in all photographs. (a) S–C fabrics in slab of Eagle Lake Tonalite which has been dated with the U–Pb zircon technique as 55 ± 3 Ma. C surfaces are parallel to the long axis of the photo; S planes dip from right (west) to left (east). (b) Slab of mylonitic orthogneiss with asymmetric pressure shadows developed around plagioclase porphyroclasts and late shear bands which dip from left to right. (c) Photomicrograph showing asymmetric pressure shadow developed around plagioclase (P) porphyroclast in chlorite–actinolite–albite schist. Short axis of photo is 3 mm; cross polarized light. (d) Retort-shaped white mica grain in metasedimentary schist, bounded by shear bands. Field of view is 2.4 x 3.6 mm; cross polarized light.

middle amphibolite grade, represented by the composite mineral assemblage biotite + muscovite + garnet + staurolite ± kyanite ± sillimanite, is of later intra- to post-Ds age. Garnet, staurolite, and kyanite overgrow Ss foliation (defined by inclusion trails) and only sometimes deflect surrounding micas. Garnet occurs as rims around rolled cores and as complete grains. Kyanite and sillimanite are confined to metapelitic rocks exposed in the central portion of the metasedimentary belt in the southern part of the study area and a small (50 m^2) pendant in the northwest part of the area. In the former area, kyanite and sillimanite were observed about 600 m and 1 km, respectively, below greenschist facies metavolcanic rocks (discussed below).

The contact between metasedimentary rocks and structurally overlying metavolcanic rocks is locally exposed in the vicinity of the pelitic schist. There chlorite + actinolite + albite ± biotite ± quartz-bearing metavolcanic rocks are juxtaposed over garnet-staurolite schist at the contact. Increasing intensity of mylonitic foliation and stretching lineation toward the contact zone indicate that significant ductile strain occurred here. The presence of kyanite ± sillimanite about 1 km below the lithologic contact and about 100 m below the associated zone of high strain suggests that metamorphic gradients are truncated or attenuated.

Metavolcanic Rocks

Metamorphic rocks thought to be derived from volcanic rocks of intermediate composition compose the structurally highest part of the DSA. They crop out in the southern part of the TLMC and as the cores of F3 synforms to the north (Figure 2a). Primary volcanic textures are lacking in these rocks which contain metamorphic chlorite + albite + biotite + quartz + amphibole (commonly actinolite). They occur as chlorite-actinolite schist and are sometimes fine grained and phyllitic in appearance. Ls, defined primarily by actinolite, is well developed, as is Ss; Fs folds occur only very rarely. Extension fractures normal to Ls are a common feature. These rocks are tentatively

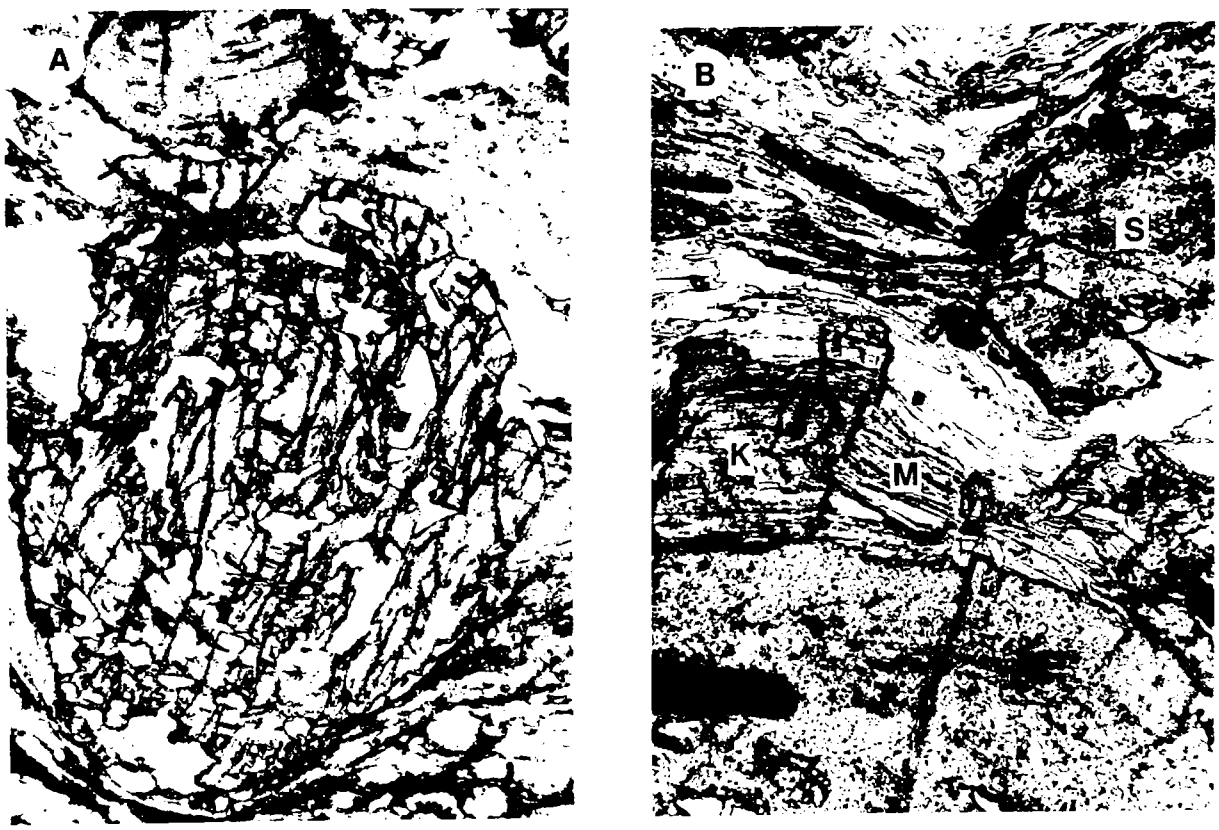

Fig. 7. Photomicrographs of metapelitic rocks in the DSA. (a) Syn-Ds rolled garnet. Short axis of photo is 2 mm; plane polarized light. (b) Kyanite (K) and staurolite (S) growing across Ss foliation. Short axis of photo is 0.5 mm; plane polarized light. (c) Staurolite (S) growing across Ss schistosity. Note Fs fold deforming schistosity in photo. Short axis of photo is 0.5 mm; plane polarized light.

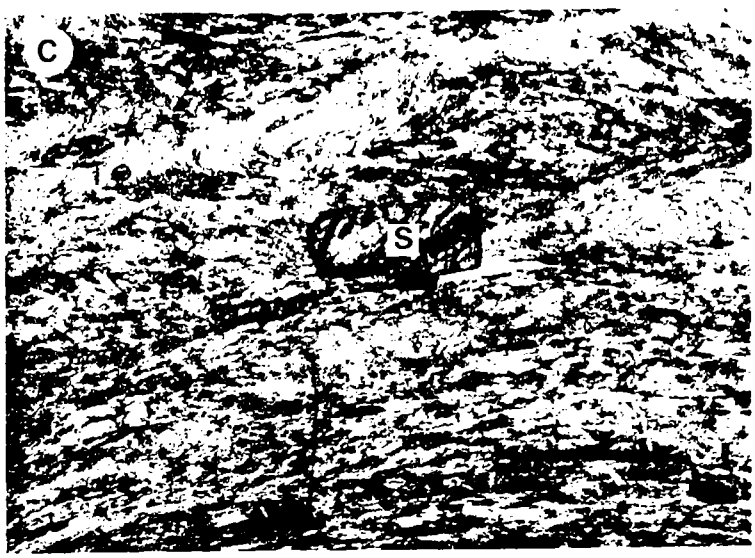

Fig. 7. (continued)

correlated with the unnamed Jurassic volcanic rocks of the IMB cover sequence (discussed below).

D3 DEFORMATION

Map- and outcrop-scale, open to normal upright folds, (F3), which affect the lower plate of the TLMC, developed during D3 deformation (Figure 2b). The regional distribution and orientation of deformed Ss (Figures 5a-5f) and S1c (Figures 4a-4c) surfaces outline map-scale F3 fold forms. F3 folds also deform F2c axial surfaces (Figures 4d and 4e). F3 fold traces curve from approximately east-west trends in the east to northwesterly adjacent to the Yalakom fault in the northwestern part of the map area (Figures 2a and 2b). Fold intensity increases from southeast to northwest across the map area.

Mesoscopic F3 structures are common in the gneissic core (especially structural subarea 8; Figure 3) and are rare elsewhere in the lower plate. They are concentric, have nearly vertically dipping axial surfaces (as do megascopic equivalents), and have no associated deformation fabrics. Mesoscopic F3 fold axes and axial surfaces are plotted on stereograms in Figures 4f and 4g.

Superposition of mesoscopic F3 upon approximately colinear F2c fold sets has resulted in the development of type 3 fold interference patterns [Ramsay, 1967]. F3 fold trends are subparallel to earlier L2c and Ls lineations throughout the map area and do not significantly deform them.

LOW-GRADE COVER ROCKS

General Discussion

Volcanic, low-grade metavolcanic and plutonic rocks occur in the IMB adjacent to the TLMC (Figures 1 and 2a). They are poorly exposed due to the subdued relief and extensive areas covered by glacial drift.

Breccia, tuff, and flows of basaltic to dacitic composition (andesites predominate) and minor sedimentary rocks are exposed directly to the south, east, and northeast of the TLMC (Figures 1 and 2a) [Tipper, 1969a, map unit 7; 1969b, map units 2 and 3]. Primary textures are preserved in these subgreenschist facies rocks which lack metamorphic foliation [Tipper, 1969a]. The presence of rare marine fossils in fine-grained tuffaceous horizons suggests that these rocks were at least in part water lain [Tipper, 1969a]. One poorly preserved ammonite found about 40 km northeast of the TLMC tentatively indicates a Bajocian age (Middle Jurassic [Tipper, 1969a]). These unnamed volcanic rocks are tentatively correlated with the Lower to Middle Jurassic Hazelton Group to the north, on the basis of similar age and lithologies.

Dacitic to rhyolitic flows reaching a maximum thickness of over 400 m are exposed 10 km northeast of the TLMC (Figures 1 and 2a). These rocks have been lithologically correlated with the Eocene Ootsa Lake volcanics which occur to the north (Figure 1) [Tipper, 1969b].

The Chilcotin Group basalts [Bevier, 1983], are

the most widely exposed rocks in the IMB adjacent to the TLMC (51°-53°N). These flows and plugs are predominantly aged 2-3 and 6-10 Ma [Bevier, 1983].

Plutonic rocks exposed southeast and east of the TLMC (Figure 1) are dominantly nonfoliated and of quartz monzonite to diorite composition [Tipper, 1969b, 1978]. Poor exposure obscures contact relations with associated Jurassic volcanic rocks. A 157 ± 5 Ma K-Ar hornblende date has been determined for a small unnamed quartz diorite body 3 km northeast of the TLMC (Table 3). The Piltz Peak granodiorite, located about 100 km east-southeast of the TLMC (Figure 1) has been assigned a minimum age of 110 Ma, based on U-Pb zircon dating (J. Monger et al., unpublished data, 1985).

Nature of Contacts With Metamorphic Core Rocks

Low-grade IMB cover rocks are in fault contact with metamorphic core rocks, based on distinct differences in structural style, metamorphic grade, and often rock type. Differences in the character of this fault (referred to as Core/Cover fault) along its length are discussed below.

The southern, east-west trending segment of the Core/Cover fault is parallel in strike to mylonitic foliation in underlying metamorphic core rocks. It places subgreenschist grade, undeformed volcanic and sedimentary rocks over greenschist facies mylonitic metavolcanic rocks (Figure 2a). About 7 km to the north, pelitic schist containing syn-Ds kyanite and sillimanite, which crystallized at a minimum depth of 10 km, is now at a maximum of 4 structural km below the Core/Cover fault (assuming a 30°-35° southerly regional dip). This structural and metamorphic omission (or attenuated metamorphic gradient) is most reasonably explained by a combination of normal ductile shear within the DSA (especially near the metadesimentary/metavolcanic contact) and normal displacement along a mylonitic-foliation-parallel fault. On the basis of these relationships the southern Core/Cover fault segment is interpreted as a syn-Ds mylonitic-foliation-parallel normal fault, with a sense of displacement similar to the underlying DSA shear zone (upper plate-to-the-west).

A poorly exposed fault which cuts a map-scale F3 fold and locally brecciates mylonitic rocks defines the northeastern and eastern margins of the TLMC lower plate (Figure 2a). The trace of this surface was determined largely by interpolating between mylonitic lower plate and low-grade upper plate rocks. The sinuosity of this fault in map view (Figure 2a) and its relationship to local topography indicate gentle to moderate east to northeasterly dips. Relatively low-grade rocks in the hanging wall provide evidence favoring down to the east normal motion.

An intersection of the southern syn-Ds Core/Cover fault segment and the north-south trending post-D3 segment (Figure 2a) is geometrically required if, as suggested, the former structure cuts up-section toward the southeast. Bedrock exposures are lacking in the vicinity where the projections of these faults meet; the syn-Ds fault is shown to truncate the post-D3 surface on Figure 2a. Another geometric consequence of the syn-Ds fault cutting up-section toward the southeast is that a breakaway (presently unrecognized) must be present in the hanging wall east of the study area. Core/Cover fault development is integrated into a model for the Eocene tectonic development of the TLMC in a later section (Figure 9).

The Yalakom fault forms the southwestern margin of the TLMC. As now exposed, it truncates both S1c gneissic layering and Ss mylonitic foliation. The latest motion is therefore post-Ds in relative age. Its age relative to D3 structures is not observable. It is thought to be steeply dipping in the study area because of its remarkably straight trace, which is expressed by a linear topographic depression 2 to 3 km wide, across which unlike rock types are juxtaposed. The Yalakom fault has not been observed north of the study area and appears to end south of 53°N (G. Woodsworth, oral communication, 1987).

GEOCHRONOMETRY

U-Pb Zircon Dates

Zircons from igneous rocks of the TLMC have yielded U-Pb and Pb-Pb dates ranging from late Jurassic through Eocene (Table 2 and Figure 8) [Friedman, 1988]. The selected U-Pb zircon dates reported here (Table 2) bracket the episodes of deformation and metamorphism in the TLMC. The dates are interpreted as crystallization ages; however, some of the fractions plot slightly off of concordia, which may be due to minor inherited zircon, Pb loss, or a combination of both effects. Pb loss is considered unlikely for samples which give zircon fractions of differing size, magnetic characteristics, and U content that are nearly coincident on a concordia plot [Chen and Moore, 1982; Saleeby, 1982].

In the gneissic core, U-Pb zircon dates bracket deformation and metamorphism of Cretaceous age. Granoblastic tonalitic orthogneiss which contains all of the structural elements observed in the gneissic core has been dated as 107 ± 3 Ma (Table 2, sample 7; Figure 8a). Two samples of the One Eye tonalite have been dated as 76 ± 3 Ma and 82 ± 3 Ma, respectively. (Table 2, samples 5 and

6; Figure 8a). A conservative estimate for the age of the One Eye Tonalite, incorporating dates and errors from both samples, is 79 ± 6 Ma. This variably but dominantly weakly foliated pluton was emplaced late in the deformational history of the gneissic core. These dates bracket much of the deformation in the gneissic core (and early metamorphism) to between 107 ± 3 Ma and 79 ± 6 Ma. These observations do not rule out the possibility that some Eocene ductile deformation occured in the gneissic core (Eocene deformation discussed below) or that other pre-Eocene episodes of deformation may have occurred there. Only favorable circumstances make it possible to bracket older deformation episodes in polydeformed rocks. In the DSA, where Eocene deformation is strongest, evidence of older events has been totally obscured.

U-Pb dates from three samples affected by ductile deformation in the DSA are reported in Table 2. Two samples from opposite ends of the Eagle Lake tonalite and one of a metadacitic sill that intrudes metasedimentary rocks have been dated as 55 ± 3 Ma (Table 2, samples 2, 3, and 4; Figure 8b). These rocks are penetratively deformed, containing regional Ss and Ls fabrics and are therefore pre- to syn-Ss/Ls. The Tatla Lake granodioritic stock, a nonfoliated body that intrudes the ductile shear zone, has been dated as 47.5 ± 1.5 Ma (Table 2, sample 1; Figure 8b). These dates bracket deformation that produced mylonitic fabrics, Fs folds, and the associated metamorphism in the ductilely sheared rocks to between 55 ± 3 Ma and 47.5 ± 1.5 Ma.

K-Ar Dates

K-Ar dates on biotite and hornblende separates have been determined for rocks from the TLMC and adjacent areas in the IMB and Coast Plutonic Belt. These dates are interpreted as the time of final cooling of the minerals through their closure temperatures [Armstrong, 1966; Dodson, 1979].

All but one of the dates from metamorphic core samples fall between 53.4 ± 1.8 Ma and 45.6 ± 1.6 Ma, interpreted as the time of uplift and rapid cooling for the TLMC (during Ds and D3 deformation). Biotite dates are between 45.6 ± 1.6 Ma and 47.5 ± 1.7 Ma (Table 3, samples 8, 9, and 12). A hornblende separate from a weakly deformed sample in the mylonitic orthogneiss unit that gave a hornblende K-Ar date of 61 ± 2 Ma (Table 3, sample 15) may have been only partially reset during Eocene time. It is not clear whether the gneissic core cooled below Ar closure temperatures between Cretaceous and Eocene metamorphic episodes or remained at high temperature until Eocene cooling. The Eocene episode has obliterated any evidence of the earlier thermal history.

Two hornblende separates from rocks adjacent to the TLMC metamorphic core have been K-Ar dated in this study. An undeformed, unnamed quartz diorite body located about 3 km northeast of the Core/Cover fault in the IMB upper plate (Figure 2a and Table 3, sample 16) was dated as 157 ± 5 Ma. A weakly foliated, unnamed quartz dioritic intrusion west of, and adjacent to, the Yalakom fault gave an age of 190 ± 7 Ma (Figure 2a and Table 3, sample 17). These dates indicate that rocks adjacent to, and in fault contact with, the TLMC metamorphic core were not heated above the Ar closure temperature for hornblende during Eocene time. U-Pb zircon and K-Ar data taken together imply that the uplift and cooling of the TLMC occurred rapidly and synchronously to slightly after the deformation and metamorphism in the ductilely sheared assemblage; during Ds and D3 deformation.

DISCUSSION

Sequence of Events

The sequence of events affecting the TLMC metamorphic core and adjacent part of the IMB are listed: (1) Lower to Middle Jurassic deposition/extrusion of stratified rocks which comprise IMB cover (Jurassic) volcanic rocks and metasedimentary/metavolcanic rocks of the TLMC metamorphic core, (2) Late Jurassic (157 Ma) through Eocene (47.5 Ma) calc-alkaline magmatism, (3) Cretaceous (107-79 Ma) metamorphism and deformation affecting rocks of the TLMC gneissic core, (4) early and middle Eocene (55-47 Ma) shear zone activity (normal, tops-to-the-west sense of motion) and metamorphism, associated with uplift, and closely followed by cooling of the TLMC lower plate rocks; Ds deformation includes the development mylonitic fabrics (Ss/Ls), Fs folds, and brittle/ductile motion along the southern segment of the Core/Cover fault, (5) D3 deformation, which includes the development of mesoscopic and map-scale F3 folds and continued uplift and cooling of lower plate rocks (syn- and/or post-47.5 Ma), and (6) post-D3 strike-slip and/or vertical motion along the Yalakom fault and down to the east normal displacement along the gently to moderately dipping eastern/northeastern Core/Cover fault.

Cretaceous Compression

Cretaceous ductile deformation (D1c± D2c) and metamorphism recorded in rocks of the gneissic core between 107 and 79 Ma are coeval with shortening recognized in a discontinuous north-northwest trending east vergent fold thrust belt located adjacent to the IMB-Coast Belt boundary between about 51° and 54°N (Mount Waddington

TABLE 2. U-Pb Zircon Isotopic Dates for the Tatla Lake Metamorphic Complex

Sample[a]	Fraction[b]	Weight, mg	U, ppm	Pb,[c] ppm	Pb Isotopic Abundance[d] ^{206}Pb=100			Observed[e] $^{206}Pb/^{204}Pb$ Ratio	$^{206}Pb/^{238}U$[f] Date, Ma	$^{207}Pb/^{235}U$ Date, Ma	$^{207}Pb/^{206}Pb$ Date, Ma
					208	207	204				
1	F,NM	5.0	2447.0	16.97	5.255	4.917	0.0129	5680	46.9 ± 0.6	47.2 ± 0.6	62.8 ± 12.8
	FF,M	10.6	3640.5	26.43	7.653	5.830	0.0726	1340	47.1 ± 0.8	47.7 ± 0.6	79.5 ± 10.2
2	C,NM	1.2	454.9	3.92	9.033	5.031	0.0391	907	55.8 ± 0.8	55.9 ± 1.6	61.7 ± 58.2
	F,M	1.8	275.0	2.29	11.288	5.550	0.0398	609	52.7 ± 0.6	55.5 ± 2.0	178.3 ± 79.0
	F,M[g]	1.3	624.9	5.41	12.112	5.903	0.0798	586	53.9 ± 0.4	54.1 ± 0.8	62.2 ± 30.8
3	F,NM	5.4	514.4	4.41	10.027	4.870	0.0093	3291	55.6 ± 0.6	55.8 ± 1.2	65.7 ± 41.6
	FF,M	4.5	651.9	5.89	14.379	5.082	0.0257	1946	56.2 ± 0.8	56.1 ± 1.4	51.1 ± 53.8
4	C,NM	7.7	473.0	4.10	13.812	5.286	0.0364	1399	54.2 ± 0.6	54.8 ± 1.0	84.7 ± 31.8
	FF,M	7.3	573.0	4.97	17.598	5.056	0.0217	2150	52.6 ± 0.6	52.9 ± 1.0	67.5 ± 37.0
5	CC,NM	10.5	166.0	2.22	17.640	5.178	0.0262	2413	80.5 ± 1.0	81.0 ± 1.0	95.4 ± 15.4
	CC,NM[g]	0.9	221.0	3.11	21.664	5.279	0.0316	646	81.9 ± 0.8	82.8 ± 2.2	106.1 ± 59.2
	C,NM[g]	4.9	202.2	2.67	17.811	5.001	0.0142	2488	79.9 ± 0.6	80.4 ± 0.8	95.6 ±11.6
6	CC,NM	8.3	173.5	2.15	16.200	5.183	0.0277	1896	75.7 ± 1.0	76.1 ± 1.0	86.4 ± 12.0
	F,M	3.8	247.3	3.12	18.980	4.853	0.0093	1316	75.5 ± 1.2	74.9 ± 2.0	57.1 ± 56.4
	C,NM[g]	5.0	195.3	2.55	19.420	6.136	0.0910	847	76.1 ± 0.6	76.7 ± 0.8	97.3 ± 19.3
7	C,NM	7.2	238.2	3.86	6.729	4.868	0.0012	4788	107.9 ± 1.4	108.6 ± 1.2	123.7 ± 9.4
	F,NM	6.3	305.3	4.98	7.321	5.031	0.0131	2989	107.7 ± 1.2	108.3 ± 1.8	121.9 ± 32.8
	FF,M	1.0	398.9	6.43	7.401	5.031	0.0131	1521	106.3 ± 1.4	106.8 ± 2.2	117.6 ± 37.8

[a] See Figure 2 for sample locations. Latitudes (N) and longitudes (W) of samples are: sample 1, Tatla Lake granodiorite 52°01.0′N, 124°23.1′W; sample 2, metadacitic sill 51°55.9′N, 124°18.7′W; sample 3, Eagle Lake tonalite 51°53.3′N, 124°17.6′W; sample 4, Eagle Lake tonalite 51°52.6′N, 124°18.2′W; sample 5, One Eye tonalite 51°56.3′N, 124°45.1′W; sample 6, One Eye tonalite 51°56.7′N, 124°46.5′W; sample 7, granoblastic orthogneiss 51°55.6′N, 124°44.9′W.

[b] CC,212-150 μm, C,150-75 μm, F,75-45 μm, FF,≤45 μm; NM,relatively nonmagnetic fraction, M,relatively magnetic fraction.

[c] Radiogenic and common Pb.

[d] Radiogenic and common Pb, corrected for 0.15% per amu fractionation and for 150±50 pg to 400±150 pg blank Pb

with the composition 208:207:206:204=37.30:15.50:17.75:1.00.

[e] Corrected for 0.15% per amu fractionation.

[f] 2σ errors reported for all dates; Decay constants: λ_{238}=0.155125x10^{-9} yr^{-1}, λ_{235}=0.98485x10^{-9} yr^{-1}; ratios are corrected for U and Pb fractionation (0.15% per amu), blank and common Pb. Isotopic compositions of Pb used for common Pb corrections from Stacey and Kramers [1975] growth curve at inferred age of each sample.

Analytical technique: zircons were separated using standard heavy mineral separation techniques. Where pyrite was present heavy silicates were further isolated using a high-voltage electrostatic separator. Fractions of single populations were selected using coventional (nylon mesh sieve) and magnetic (Franz isodynamic separator) separations, followed by handpicking to virtually 100% purity. Sample dissolution and chemistry were carried out using a procedure modified from Krogh [1973]. U and Pb concentrations were determined using a mixed ^{208}Pb/^{235}U spike. Purified U and Pb were loaded on Re filaments using H_3PO_4-silica gel technique. Mass spectrometric analysis was carried out using a VG Isomass 54R solid source mass spectrometer in single collector mode (Faraday cup). Precisions for ^{207}Pb/^{206}Pb and ^{208}Pb/^{206}Pb were less than 0.2% and for ^{204}Pb/^{206}Pb were less than 3%. Pb/U and Pb/Pb errors for individual zircon fractions were obtained by individually propagating all calibration and analytical uncertainties through the entire date calculation program and summing the individual contributions to the total variance.

[g] U and Pb concentrations determined using a mixed ^{208}Pb/^{235}U spike.

map sheet (92N) [Tipper, 1969a; Rusmore and Woodsworth, 1988]; Warner Pass map sheet (92O/3) [Glover and Schiarizza 1987]; Whitesail Lake map sheet (93E) [van der Heyden, 1982]). Cretaceous thrusting is thought to be responsible for crustal thickening and the burial of the TLMC lower plate, including Jurassic (?) supracrustal rocks. Kyanite-bearing metapelitic rocks of the DSA were at a minimum depth of 10 km during Eocene Ds deformation.

Eocene Tectonic Development of the TLMC

The Eocene tectonic development of the TLMC is depicted in a series of schematic east-west cross sections in Figure 9. The dominant operative structural element in the TLMC during Ds deformation (55–47.5 Ma) was a gently westward dipping ductile and brittle normal fault zone (Figure 9a). Mylonitic rocks of the DSA developed at deeper levels in the active tops-to-the-west normal shear zone. The transport of mylonitic rocks to shallower crustal levels within this ductile/brittle fault zone accounts for structural and metamorphic omission (or attenuation of metamorphic gradient) documented along the southern Core/Cover fault and in adjacent metavolcanic and metasedimentary rocks.

The presence of texturally late porphyroblasts in DSA pelitic schist from the southern part of the lower plate (garnet, staurolite, and especially kyanite; Figures 7b and 7c) is difficult to explain in the context of a shoaling ductile/brittle fault zone. A reasonable hypothesis is that strain largely abated in these porphyroblast-bearing rocks prior to the end of Ds deformation; during the later stages of Ds deformation, strain was concentrated in narrow anastamosing shear zones around lenticular bodies, such as the areas sampled, where earlier fabrics are preserved.

While normal motion within the ductile/brittle fault depicted in Figure 9a accounts for most of the structure of the TLMC lower plate and part of its uplift, final uplift and exhumation of these rocks is thought to postdate activity along that system. Post-47.5 Ma K-Ar cooling dates (Table 3) indicate that uplift and cooling occurred after deformation ceased in the TLMC shear zone; part of the uplift may be related to D3 deformation. D3 deformation is hypothesized to be the result of transpression at a restraining bend along the dextral transcurrent Yalakom fault. This is based on the geometry of map-scale F3 folds as shown on the map in Figure 2a and the schematic diagram in Figure 10. These folds curve into parallelism with the trace of the Yalakom fault and are best developed adjacent to it. Transpressive crustal thickening and consequent uplift would be predicted to increase toward the Yalakom fault. Figure 9b is a schematic east-west cross section set at the end of D3 deformation. The then inactive ductile shear

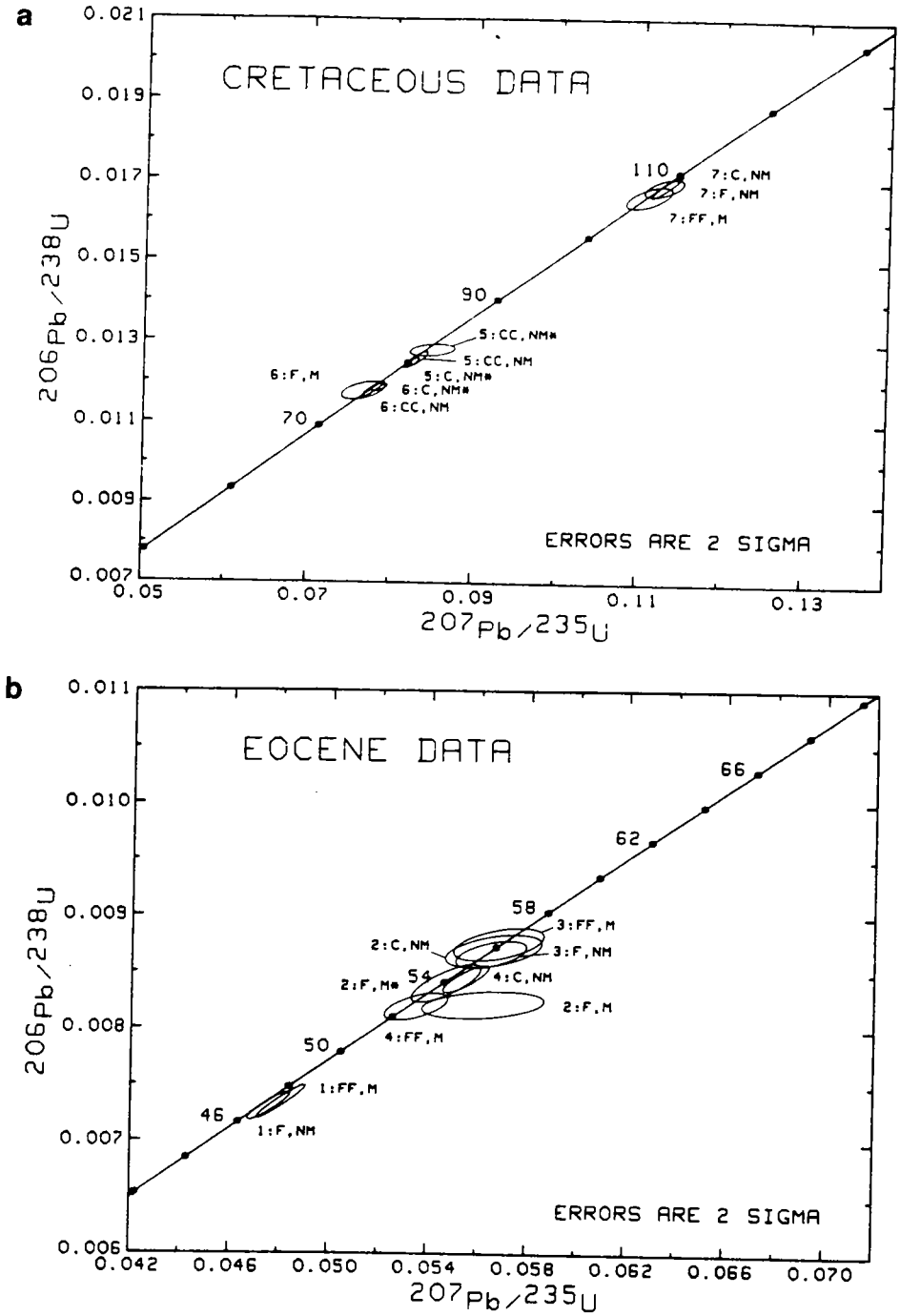

Fig. 8. U–Pb concordia plots for zircons from the TLMC. Analytical data are listed in Table 2, and sample locations are plotted on Figure 2a. Asterisks indicate samples that have been run with ^{205}Pb spike (post-1986). (a) Cretaceous data. (b) Eocene data.

zone had been deformed by F3 folds and was at high crustal levels and perhaps exposed to erosion.

Figure 9c shows the TLMC when the eastern-northeastern Core/Cover fault was active. The topology of this cross section is similar to structures observed today. Upper and lower plate rocks are juxtaposed along the eastern/northeastern Core/Cover and Yalakom faults.

TABLE 3. K-Ar Dates for the Tatla Lake Metamorphic Complex

Sample[a]	Name	Material Analyzed	Percent K	Percent Radiogenic ^{40}Ar	Radiogenic ^{40}Ar x 10^{-6} cm^3/g	Date, Ma[b]
8	metadacitic sill	biotite	7.11	90.6	13.254	47.3 ± 1.7
9	Eagle Lake tonalite	biotite	7.59	91.5	14.210	47.5 ± 1.7
10	granoblastic gneiss	hornblende	0.776	49.0	1.470	48.1 ± 1.7
11	metavolcanic	hornblende	0.424	49.9	0.766	45.9 ± 1.6
12	granodioritic sill	biotite	7.46	79.4	13.384	45.6 ± 1.6
13	granoblastic gneiss	hornblende	0.655	76.3	1.197	46.4 ± 1.6
14	granoblastic gneiss	hornblende	0.483	45.2	1.017	53.4 ± 1.8
15	orthogneiss	hornblende	0.414	54.8	0.998	61.0 ± 2.0
16	quartz diorite	hornblende	0.478	90.1	3.038	157.0 ± 5.0
17	quartz diorite	hornblende	0.298	88.3	2.231	190.0 ± 7.0

[a] See Figure 2 for sample locations. Latitudes(N) and longitudes(W) of samples are: sample 8, 51°55.9′N, 124°18.7′W; sample 9, 51°53.3′N, 124°17.6′W; sample 10, 51°58.9′N, 124°33.1′W; sample 11, 51°57.4′N, 124°40.5′W; sample 12, 51°51.8′N, 124°34.3′W; sample 13, 51°55.6′N, 124°44.9′W; sample 14, 52°00.6′N, 124°50.3′W; sample 15, 52°03.7′N, 124°53.0′W; sample 16, 52°02.7′N, 124°33.8′W; sample 17, 51°49.7′N, 124°42.0′W.

[b] 1σ errors reported for all dates.

Analyses by K. Scott (K) and J. Harakal (Ar) at the Department of Geological Sciences, University of British Columbia. K is determined in duplicate by atomic absorption using a Techtron AA4 spectrophotometer and Ar by isotope dilution using an AEI MS-10 mass spectrometer, high purity ^{38}Ar spike, and conventional gas extraction and purification procedures [White et al., 1967]. The constants used are $\lambda^{40}Ke=0.581\times10^{-10}$ yr^{-1}, $\lambda^{40}K\beta=4.962\times10^{-10}$ yr^{-1}, $^{40}K/K=0.01167$ at. %.

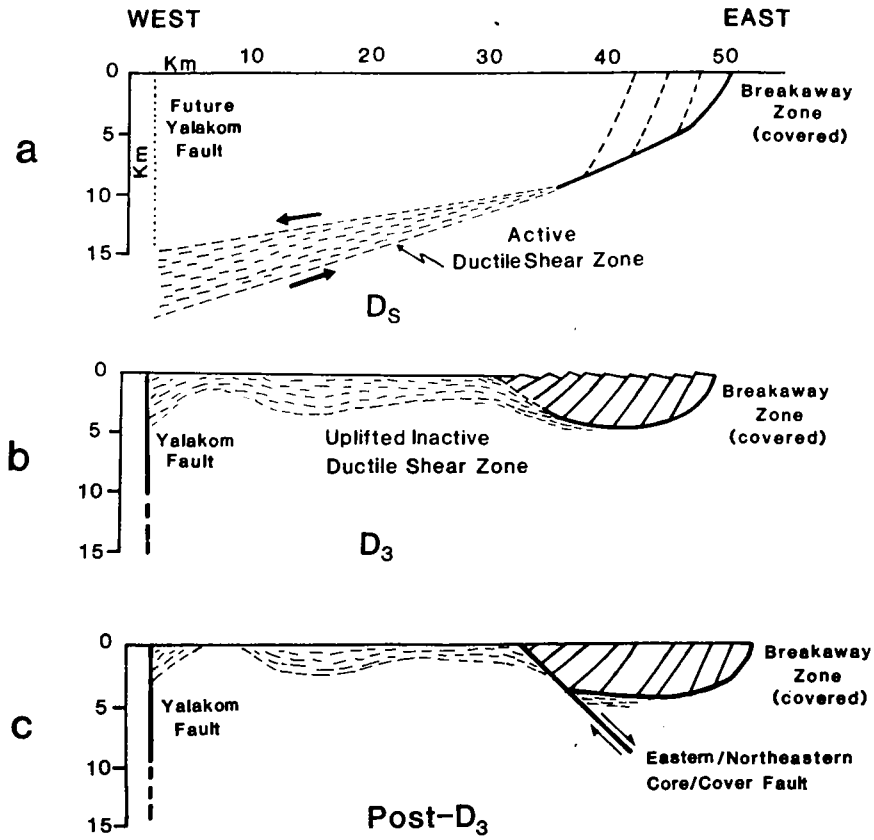

Fig. 9. Schematic east-west cross sections depicting the early to middle Eocene and later Tertiary tectonic development of the TLMC. Dashed pattern represents mylonitic and ductilely sheared metamorphic rocks. See text for details. (a) West dipping normal ductile and brittle fault zone active during Ds deformation (55–47.5 Ma). Rocks of the DSA were deformed in the active ductile shear zone shown in this section. (b) Uplifted, inactive shear zone folded by F3 folds during the late stages of D3 deformation (post–47 Ma); synchronous with early movement on the Yalakom fault. (c) Post-D3 movement along the eastern/northeastern Core/Cover fault, along which upper and lower plate rocks are juxtaposed; Yalakom fault present but amount of movement undefined.

Eocene Extensional Deformation in Southern British Columbia and the Northwestern United States

Early to middle Eocene crustal extension and rapid uplift/cooling of deeper crustal metamorphic rocks have been documented in Cordilleran metamorphic core complexes in southeastern British Columbia, northeastern Washington, and northern Idaho [Cheney, 1980; Armstrong, 1982; Parrish, 1984; Carr, 1985; Parkinson, 1985; Rhodes, 1986; Carr et al., 1987, Parrish et al., 1988]. Structural studies indicate an approximate east-west extension direction throughout these core complexes and tops-to-the-west sense of shear along their westernmost sides [Armstrong, 1982; Parkinson, 1985; Wust, 1986]. Eocene ductile deformation with near-horizontal intermediate and maximum elongation axes has been observed in the Bridge River Terrane of southwestern British Columbia, where deformed igneous rocks have been dated as 41–45 Ma [Potter, 1986] (U-Pb zircon dates of J. Monger and P. van der Heyden personal communication, 1987). Farther south, in the North Cascades of Washington and British Columbia, U-Pb (45 Ma [Haugerud et al., 1988]) and Rb-Sr data (whole rock isochron, 45 Ma [Babcock et al., 1985]) from ductilely deformed rocks of the Ross Lake Shear Zone indicate an Eocene time of movement within this structural zone (including differential uplift [Haugerud, 1985]). Eocene K-Ar and Rb-Sr mica dates tightly clustered at 45–50 Ma give the time of uplift and final cooling for southern British Columbia and northwestern U.S. Cordilleran metamorphic core complexes [Armstrong, 1974, 1975, 1976, 1988; Ross, 1974; Medford, 1975; Miller and Engels, 1975; Fox et al., 1977;

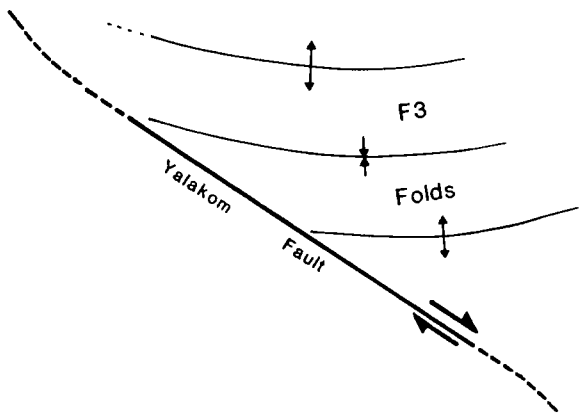

Fig. 10. Schematic diagram showing D3 transpression localized at a minor restraining bend in the Yalakom fault (post-47.5 Ma). D3 deformation is thought to be responsible for final uplift and cooling of the lower plate.

Mathews, 1981; Parrish et al., 1988], the Nicola Batholith [Preto et al., 1979; Ewing, 1980], the North Cascades [Misch, 1964; Engels et al., 1976], and Bridge River areas [Potter, 1983; R. L. Armstrong, unpublished data, 1983].

TLMC and Eocene Regional Tectonics of Southern British Columbia and Northern Washington

Overthickened, thermally weakened crust and a change of plate motions in the northeastern Pacific region have been cited as general causes of Eocene extensional deformation in southeastern British Columbia and northern Washington (from Parrish et al. [1988], following the general extensional model of Sonder et al. [1987]). Similar argurments may also apply to coeval extension documented in the TLMC. There, thermal weakening of the crust was probably primarily related to Eocene magmatism, as it was situated in the central portion of a wide and vigorous magmatic belt (Figure 12) [Armstrong, 1988]. Tectonic thickening may have also played a role in thermally weakening the crust and in creating the potential for later extension in the TLMC area. An easterly verging Cretaceous fold thust system located near the Coast Belt-IMB boundary [Tipper, 1969a; Rusmore and Woodsworth, 1988; van der Heyden, 1982; Glover and Schiarizza, 1987] could have caused or been related to this thickening. High-level thrusts in this system are presently exposed directly to the west of the study area. High-level thrusts that may have overlain the TLMC at the time of D1c and D2c deformation could have been removed during Eocene Ds and D3 deformation, uplift, and erosion. Moreover, Cretaceous crustal shortening occurred throughout the Intermontane Belt, as shown by deformed Cretaceous rocks of the Methow-Tyaughton basin [Kleinspehn, 1985; Ray, 1986] and Bowser and Sustut basins [Eisbacher, 1974; Moffat, 1985; Evenchick, 1987, 1988] and K-Ar dating of deformed Hazelton and Bowser Lake Group volcanic and sedimentary rocks [Alldrick et al., 1987; Devlin, 1987].

The external cause of Eocene extension listed above, a change in plate motions in the northeastern Pacific region, is thought to have resulted in oblique northward motion of the Farallon plate relative to North America [Londsdale, 1988; Engebretson et al., 1985]. This external tectonic change could have been responsible for a reduction in stress exerted normal to the North American plate, which, when coupled with magmatic weakening of thickened crust, could have resulted in widespread extension in southwestern Canada and the northwestern United States.

A more specific kinematic model for Eocene extension in southeastern British Columbia has been proposed by Price [1979] and Price and Carmichael [1986]. They envisaged Eocene crustal stretching in the southern IMB occurring in a right step from the Fraser-Straight Creek (F-Sc) to the Northern Rocky Mountain Trench-Tintina (NRMT-T) dextral fault systems. This model can geometrically explain extension in large areas of southern British Columbia, but as shown on Figure 11, the region between the en echelon Fraser and NRMT-T fault systems is not large enough to account for Eocene ductile extension documented in all the Eocene metamorphic core complexes of the northwestern United States, or those west of the Fraser fault.

In addition to the geometrical problem discussed above, the time of motion along the F-Sc fault system largely postdates ductile extensional deformation in the TLMC and other Pacific Northwest core complexes. Deformed granitic dykes dated as 45 Ma (U-Pb zircon, xenotime [Haugreud et al., 1988; P. van der Heyden, unpublished data, 1987]) provide the minimum age of ductile deformation in the Ross Lake Shear Zone and a maximum age for motion along the crosscutting brittle F-Sc fault system. Two reverse faults which are interpreted as splays of the Fraser fault have also been assigned middle or late Eocene maximum ages. The Phair Creek fault, located southwest of Lillooet (Figure 1), places upper Triassic rocks over a middle Eocene igneous body (U-Pb zircon date of 47 Ma [Monger, 1982, 1985]). Farther north, between the Yalakom and Fraser faults (Figure 1), motion along the Hungry Valley fault must postdate the late Eocene age of strata which it cuts [Mathews and Rouse, 1984]. A 35 Ma minimum age of motion along the F-Sc system is provided by the oldest dated phase of the Chilliwack Batholith (Silver Creek Stock [Richards and McTaggart, 1976]), which intrudes the fault zone.

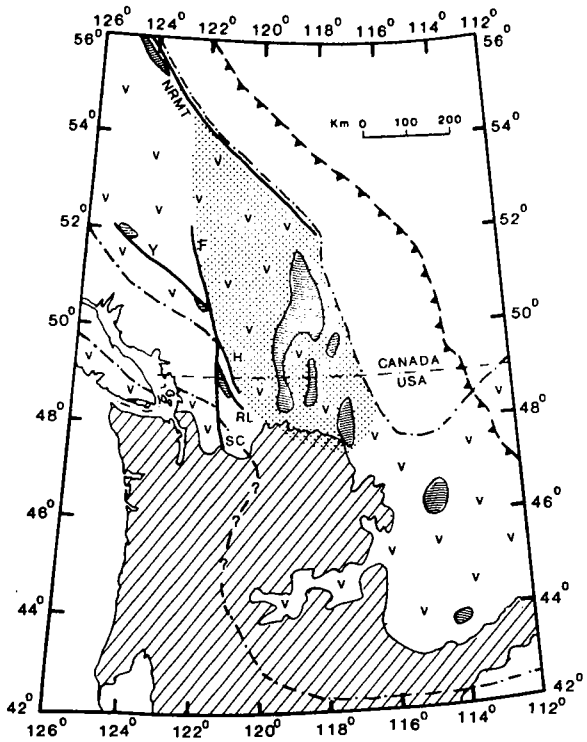

Fig. 11. Map of southwestern Canada and the northwestern United States showing the distribution of Eocene metamorphic core complexes and the areal extent of the Paleogene magmatic arc. Eocene metamorphic core complexes, closely spaced, wavy, and subhorizontal ruled pattern; magmatic arc, "v" pattern, bounded by dot-dashed lines; area in the right step between the dextral NRMT and F-Sc fault systems where extension (transtension) would be predicted [Price and Carmichael, 1986], stippled pattern; Tertiary rocks of the Washington and Oregon Coast Ranges and southernmost Vancouver Island, and post-Eocene cover, diagonal ruled lines; H, Hozameen fault; NRMT, Northern Rocky Mountain Trench fault; RL, Ross Lake Shear Zone; SC, Strait Creek fault; Y, Yalakom fault. Two apparently separate magmatic belts are shown on this figure. The minor western belt occurs on Vancouver Island and in the western foothills of the Northern Cascade Mountains. The western boundary of the main magmatic belt is offset by the F-Sc fault system.

The general model for extension discussed above, which involves thermal weakening of the crust as a result of magmatism in areas that had previously undergone tectonic thickening, coupled with external tectonic change, is perhaps the most satisfactory explanation for Eocene extensional deformation. Thermal weakening of the crust is supported by the observation that exposures of Eocene ductilely stretched rocks in British Columbia and the northwestern United States lie within the coeval volcano-plutonic arc (Figure 11) and that most core complexes occur in areas that were tectonically thickened during Cretaceous and Paleocene compressional deformation. This leads to the hypothesis that a regional ductile shear zone (presently largely unexposed) formed within the crust of the southern IMB during early to middle Eocene time. This idea is illustrated in a crustal cross section containing the TLMC and southeastern British Columbia core complexes (Figure 12, discussed below).

At the time of ductile stretching, before displacement on the Fraser fault system, the TLMC would have been opposite the central part of the Shuswap Metamorphic Complex. Its reconstructed position is the basis for Figure 12, not its present position north of the Intermontane and Omineca Belt areas most affected by Eocene crustal extension. The similar fabrics, stretching direction, sense of shear, and age of the TLMC and structures along the western side of the Omineca Belt invite the hypothesis that both are related parts of a regional ductile stretching zone. As shown in the section in Figure 12, the TLMC shear zone roots into a regional ductile shear zone which extends eastward across the IMB (the width of the early to middle Eocene magmatic arc), connecting with structures that emerge along the west side of the Omineca Belt. Although this regional shear zone is hypothetical, it is subject to future testing. If an Eocene ductile shear zone underlies the southern IMB, then mylonitic foliated and tectonically banded rock may be observed across the entire IMB on deep seismic reflection profiles. In the United States Cordillera many seismic profiles in the hinterland of the Mesozoic foreland fold and thrust belt show gently dipping reflectors expressing a layered lower crust that has been interpreted to be mylonite or tectonically interlayered rocks [Smithson et al., 1979; Allmendinger et al., 1983, 1987; Fountain et al., 1984; Potter et al., 1986]. Examples of areas where flat reflectors at middle to lower crustal levels have been inferred to be Cenozoic mylonitic or tectonically banded rocks include the Basin and Range Province of the western Utah and eastern Nevada [Allmendinger et al., 1983; Klemperer et al., 1986] and the Okanogan region of northern Washington [Potter et al., 1986]. We predict that LITHOPROBE transects connecting the subduction zone imaged on Vancouver Island [Yorath et al., 1985] with the core complex to Rocky Mountains fold and thrust belt line of southeastern British Columbia [Cook et al., 1988], may likewise observe an extensive shear zone in the lower crust beneath the southern IMB. The significance of the TLMC is that it affords access to rocks that could be middle to lower crust seismic energy reflecting

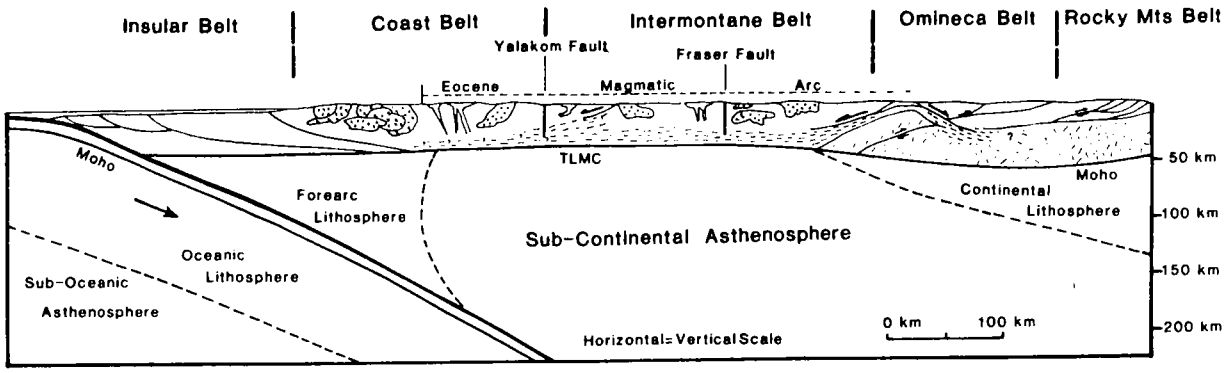

Fig. 12. Schematic Eocene east-west Cordilleran cross section (circa 55-47.5 Ma) through the TLMC restoring approximately 100 km of dextral motion along the Fraser fault system (with apologies to Monger et al. [1985]). Dashed pattern, North American continental basement; crossed pattern, Mesozoic plutonic rocks; TLMC, Tatla Lake Metamorphic Complex; bold and fine arrows denote Eocene and Mesozoic movement directions, respectively.

horizons so that the nature and ages of those reflectors can be directly examined rather than inferred.

A quotaton from Barrell [1915, p. 515] in a prescient discussion of the strength of the earth's crust is perhaps appropriate:

> At greater depths the rock is still more compressed, and is still more rigid than above, but the temperature here approaches fusion; recrystallization readily takes place, the strain which can be elastically carried is in consequence low, and the lithosphere passes gradually into the asthenosphere. Where, however magmas rise through the crust they carry with them the environment of the asthenosphere; the lithosphere becomes locally abnormally heated and saturated with magmatic emanations. Recrystallization goes foward readily and the zone of weakness penetrates upward even to the zone of fracture. Thus in the injected and crystallized roofs of ancient batholiths, laid bare by profound erosion, we may perceive the nearest approach to dynamic conditions which prevail in depths forever hidden.

Acknowledgments. We would like to acknowledge H. Trenchard and A. Jung for assistance in the field; K. Scott, J. Harakal, P. van der Heyden, J. K. Mortensen, and D. L. Parkinson for help in the laboratory; and R. R. Parrish, R. A. Price, J. W. H. Monger, W. H. Mathews, G. J. Woodsworth, J. A. Fillipone, H. W. Tipper, P. van der Heyden, J. O. Wheeler, and H. Gabrielse for discussion of geology and review of the manuscript. Funding for this project came from NSERC grant A-8841 to R. L. Armstrong.

REFERENCES

Alldrick, D. J., D. A. Brown, J. E. Harakal, J. K. Mortensen, and R. L. Armstrong, Geochronology of the Stewart mining camp (104B/1), in *Geological Research 1986, Pap. 1987-1*, pp. 81-92, British Columbia Minist. of Energy, Mines and Pet. Resour., Victoria, 1987.

Allmendinger, R. W., J. W. Sharp, D. von Tish, L. Serpa, L. Brown, S. Kaufman, J. Oliver, and R. B. Smith, Cenozoic and Mesozoic structure of the eastern Basin and Range province, Utah, from COCORP seismic-reflection data, *Geology, 11*, 532-536, 1983.

Allmendinger, R. W., K. D. Nelson, C. J. Potter, M. Barazangi, L. D. Brown, and J. E. Oliver, Deep seismic reflection characteristics of the continental crust, *Geology, 15*, 304-310, 1987.

Armstrong, R. L., K-Ar dating of plutonic and volcanic rocks in orogenic belts, in *Potassium-Argon Dating*, edited by O. A. Shaeffer and J. Zähringer, pp. 117-133, Springer-Verlag, New York, 1966.

Armstrong, R. L., Geochronometry of the Eocene volcanic-plutonic episode in Idaho, *Northwest Geol., 3*, 1-15, 1974.

Armstrong, R. L., The geochronometry of Idaho, *Isochron/West, 14*, 1-50, 1975.

Armstrong, R. L., The geochronometry of Idaho, *Isochron/West, 15*, 1-33, 1976.

Armstrong, R. L., Cordilleran metamorphic core complexes — From Arizona to southern Canada, *Annu. Rev. Earth Planet. Sci., 10*, 129-154, 1982.

Armstrong, R. L., Mesozoic and early Cenozoic magmatic evolution of the Canadian Cordillera, *Spec. Pap. Geol. Soc. Am.*, 218, 55-91, 1988.

Babcock, R. S., R. L. Armstrong, and P. Misch,

Isotopic constraints on the age and origin of the Skagit Metamorphic Suite and related rocks, *Geol. Soc. Am. Abstr. Programs, 17*, 339, 1985.

Baer, A. J., Bella Coola – Laredo Sound map-areas, British Columbia, *Mem. Geol. Surv. Can., 372*, 122 pp., 1973.

Barrell, J., Physical conditions controlling the nature of the lithosphere and asthenosphere, part VIII, The strength of the Earth's crust, *J. Geol., 23*, 424–515, 1915.

Bell, T. H., Progressive deformation and reorientation of fold axes in a ductile mylonite zone: The Woodroffe Thrust, *Tectonophysics, 44*, 285–320, 1978.

Bell, T. H., and R. L. Hammond, On the internal geometry of mylonite zones, *J. Geol., 92*, 667–686, 1984.

Bevier, M. L., Regional stratigraphy and age of the Chilcotin Group basalts, south-central British Columbia, *Can. J. Earth Sci., 20*, 515–524, 1983.

Carr, S. D., Ductile shearing and brittle faulting in Valhalla gneiss complex, southeastern British Columbia, Current Research, Part A, *Geol. Surv. Can., Pap. 85-1A*, 89–96, 1985.

Carr, S. D., R. R. Parrish, and R. L. Brown, Eocene structural development of the Valhalla Complex, southeastern British Columbia, *Tectonics, 6*, 175–196, 1987.

Chen, J. H., and J. G. Moore, U-Pb istopic ages from the Sierra Nevada Batholith, California, *J. Geophys. Res., 87*, 4761–4784, 1982.

Cheney, E. S., Kettle dome and related structures in northeastern Washington, *Mem. Geol. Soc. Am., 153*, 463–483, 1980.

Christie, J. M., The Moine thrust zone in the Assynt region, northwest Scotland, *Univ. Calif. Berkeley Publ. Geol. Sci., 40*, 245–319, 1963.

Coney, P. J., Cordilleran metamorphic core complexes: An overview, *Mem. Geol. Soc. Am., 153*, 7–31, 1980.

Cook, F. A., A. G. Green, P. S. Simony, R. A. Price, R. R. Parrish, B. Milkereit, P. L. Gordy, R. L. Brown, K. C. Coflin, and C. Patenaude, Lithoprobe seismic reflection structure of the southeastern Canadian cordillera: Initial results, *Tectonics, 7*, 157–180, 1988.

Dawson, G. M., Report on explorations in British Columbia, *Prog. Rep. 1875-1876*, pp. 233–265, Geol. Surv. of Can., Ottawa, Ont., 1876.

Devlin, B. D., Geology and genesis of the Dolly Varden silver camp, Alice Arm area, northwestern British Columbia, M.Sc. thesis, 131 pp., Univ. of British Columbia, Vancouver, 1987.

Dodson, M. H., Theory of cooling ages, in *Lectures in Isotope Geology*, edited by E. Jäger and J. C. Hunziker, pp. 195–202, Springer-Verlag, New York, 1979.

Dolmage, V., Tatla-Bella Coola area, Coast District, British Columbia, *Summ. Rep., 1925, Part A*, pp. 155–163, Geol. Surv. of Can., Ottawa, Ont., 1926.

Eisbacher, G. H., Deltiac sedimentation in the northeastern Bowser basin, British Columbia, *Geol. Surv. Can., Pap. 73-33*, 13 pp., 1974.

Engebretson, D. A., A. Cox, and R. R. Gordon, Relative motion between oceanic and continental plates in the Pacific basin, *Spec. Pap. Geol. Soc. Am., 206*, 55 pp., 1985.

Engels, J. C., R. C. Tabor, F. K. Miller, and J. D. Obradovich, Summary of K-Ar, Rb-Sr, U-Pb, Pbα, and fission-track ages of rocks from Washington State prior to 1975, *U.S. Geol. Surv. Misc. Field Study Map, MF-710*, 1976.

Evenchick, C. A., Stratigraphy and structure of the northeast margin of the Bowser basin, Spatsizi map area, north-central British Columbia, Current Research, Part A, *Geol. Surv. Can., Pap. 87-1A*, 719–726, 1987.

Evenchick, C. A., Structural style and stratigraphy in northeast Bowser and Sustut basins, north-central British Columbia, Current Research, Part E, *Geol. Surv. Can., Pap. 88-1E*, 91–95, 1988.

Ewing, T. E., Paleogene tectonic evolution of the Pacific northwest, *J. Geol., 88*, 619–638, 1980.

Fountain, D. M., C. A. Hurich, and S. B. Smithson, Seismic reflectivity of mylonite zones in the crust, *Geology, 12*, 195–198, 1984.

Fox, K. F., C. D. Rinehart, and J. C. Engels, Plutonism and orogeny in north-central Washington – Timing and regional context, *U.S. Geol. Surv. Prof. Pap., 989*, 27 pp., 1977.

Friedman, R. M., Geology and geochronometry of the Eocene Tatla Lake Metamorphic Core Complex, western edge of the Intermontane Belt, British Columbia, Ph.D. thesis, 348 pp., Univ. of British Columbia, Vancouver, 1988.

Gabites, J. E., Geology and geochronometry of the Cogburn Creek-Settler Creek area, northeast of Harrison Lake, British Columbia, M.Sc. thesis, 153 pp., Univ. of British Columbia, Vancouver, 1985.

Glover, J. K. and P. Schiarizza, Geology and mineral potential of the Warner Pass map sheet (92O/3), in *Geological Research in 1986, Pap. 1987-1*, pp. 157–169, British Columbia Minist. of Energy, Mines and Pet. Resour., Victoria, 1987.

Hansen, E., *Strain Facies*, 207 pp., Springer-Verlag, New York, 1971.

Haugerud, R. A., Geology of the Hozameen Group and the Ross Lake Shear Zone, Maselpanik area, North Cascades, southwest British Columbia, Ph.D. thesis, 263 pp., Univ. of Wash., Seattle, 1985.

Haugerud, R. A., R. W. Tabor, J. Stacey, and P. van der Heyden, What is the core of the North Cascades?, *Geol. Soc. Am. Abstr. Programs, 20*, 168, 1988.

Kleinspehn, K. L., Cretaceous sedimentation and tectonics, Tyaughton-Methow Basin, southwestern British Columbia, *Can. J. Earth Sci., 22*, 154-174, 1985.

Klemperer, S. L., T. A. Hague, E. C. Hauser, J. E. Oliver, and C. J. Potter, The Moho in the northern Basin and Range province, Nevada, along the COCORP 40°N seismic-reflection transect, *Geol. Soc. Am. Bull., 97*, 603-618, 1986.

Krogh, T. E., A low contamination method for hydrothermal decomposition of zircon and extraction of U and Pb for isotopic age determinations, *Geochim. Cosmochim. Acta, 37*, 485-494, 1973.

Lister, G. S., and A. W. Snoke, S-C mylonites, *J. Struct. Geol., 6*, 617-638, 1984.

Londsdale, P., Paleogene history of the Kula plate: Offshore evidence and onshore implications, *Geol. Soc. Am. Bull., 100*, 733-754, 1988.

Mathews, W. H., Early Cenozoic resetting of potassium-argon dates and geothermal history of the northern Okanagan area, British Columbia, *Can. J. Earth Sci., 18*, 1310-1319, 1981.

Mathews, W. H., and G. E. Rouse, The Gang Ranch – Big Bar area, south-central British Columbia: Stratigraphy, geochronology, and palynology of the Tertiary beds and their relationship to the Fraser fault, *Can. J. Earth Sci., 21*, 1132-1144, 1984.

Medford, G. A., K-Ar and fission track geochronometry of an Eocene thermal event in the Kettle River (west half) map-area, southern British Columbia, *Can. J. Earth Sci., 12*, 836-843, 1975.

Miller, F. K., and J. C. Engels, Distribution and trends of discordant ages of the plutonic rocks of northwestern Washington and northern Idaho, *Geol. Soc. Am. Bull., 86*, 517-528, 1975.

Misch, P., Age determinations on crystalline rocks of the Northern Cascades Mountains, Washington, in *Investigations in Isotopic Geochemistry, United States At. Energy Comm. Pub. NYO-7243*, edited by J. L. Kulp et al., Appendix D, pp. 1-15, Columbia University, Lamont-Doherty Geological Observatory, Palisades, N.Y., 1964.

Moffat, I., The nature and timing of deformational events and organic and inorganic metamorphism in the northern Groundhog coalfield: Implications for the tectonic history of the Bowser basin, Ph.D. thesis, 205 pp., Univ. of British Columbia, Vancouver, 1985.

Monger, J. W. H., Geology of Ashcroft map area, southwestern British Columbia, Current Research, Part A, *Geol. Surv. Can., Pap. 82-1A*, 293-297, 1982.

Monger, J. W. H., Structural evolution of the southwestern Intermontane Belt, Ashcroft and Hope map-areas, British Columbia, Current Research, Part A, *Geol. Surv. Can., Pap. 85-1A*, 349-358, 1985.

Monger, J. W. H., R. M. Clowes, R. A. Price, P. S. Simony, R. P. Riddihough, and G. J. Woodsworth, Juan de Fuca plate to Alberta plains, *Continent Ocean Transect 7*, Geol. Soc. of Am., Boulder, Colo., 1985.

Parkinson, D. L., U-Pb geochronometry and regional geology of the southern Okanagan valley, British Columbia: Western boundary of a metamorphic core complex, M.Sc. thesis, 149 pp., Univ. of British Columbia, Vancouver, 1985.

Parrish, R. R., Slocan Lake fault: A low angle fault zone bounding the Valhalla gneiss complex, Nelson map-area, southern British Columbia, Current Research, Part A, *Geol. Surv. Can., Pap. 84-1A*, 323-330, 1984.

Parrish, R. R., S. D. Carr, and D. L. Parkinson, Eocene extensional tectonics and geochronology of the southern Omineca Belt, southern British Columbia and Washington, *Tectonics, 7*, 181-212, 1988.

Potter, C. J., Geology of the Bridge River Complex, southern Shulaps Range, British Columbia: A record of Mesozoic convergant tectonics, Ph.D. thesis, 192 pp., Univ. of Wash., Seattle, 1983.

Potter, C. J., Origin, accretion, and postaccretionary evolution of the Bridge River Terrane, southwest British Columbia, *Tectonics, 5*, 1027-1041, 1986.

Potter, C. J., W. E. Sanford, T. R. Yoos, E. I. Prussen, R. W. Keach II, J. E. Oliver, S. Kaufman, and L. D. Brown, COCORP deep seismic reflection traverse of the interior of the North American Cordillera, Washington and Idaho: Implications for orogenic evolution, *Tectonics, 5*, 1007-1025, 1986.

Preto, V. A., M. J. Osatenko, W. J. McMillan, and R. L. Armstrong, Isotopic dates and strontium isotopic ratios for plutonic and volcanic rocks in the Quesnel Trough and Nicola Belt, south-central British Columbia, *Can. J. Earth Sci., 16*, 1658-1672, 1979.

Price, R. A., Intracontinental ductile crustal spreading linking the Fraser River and northern Rocky Mountain trench transform fault zones, south-central British Columbia and northeast Washington, *Geol. Soc. Am. Abstr. Programs, 11*, 499, 1979.

Price R. A., and D. M. Carmichael, Geometric test of Late Cretaceous-Paleogene intracontinental transform faulting in the Canadian Cordillera, *Geology, 14*, 468-471, 1986.

Ramsay, J. G., *Folding and Fracturing of Rocks*, 568 pp., McGraw-Hill, New York, 1967.

Ray, G. E., The Hozameen fault system and related Coquihalla serpentine belt of southwestern British Columbia, *Can. J. Earth Sci., 23*, 1022-1041, 1986.

Rhodes, B. P., Metamorphism of the Spokane dome mylonitic zone, Priest River Complex: Constraints on the tectonic evolution of northeastern Washington and northern Idaho, *J. Geol., 94*, 539–556, 1986.

Richards, T. A., and K. C. McTaggart, Granitic rocks of the southern Coast Plutonic Complex and the northern Cascades of British Columbia, *Geol. Soc. Am. Bull., 87*, 935–953, 1976.

Ross, J. V., A Tertiary thermal event in south-central British Columbia, *Can. J. Earth Sci., 11*, 1116–1122, 1974.

Rusmore, M. E., Geology and tectonic significance of the Upper Triassic Cadwallader Group and its bounding faults, southwestern British Columbia, Ph.D. thesis, 174 pp., Univ. of Wash., Seattle, 1985.

Rusmore, M. E. and Woodsworth, G. J., Eastern margin of the Coast Plutonic Complex, Mount Waddington map area (92N), British Columbia, in Current Resaerch, Part E, *Geol. Surv. Can., Pap. 88-1E*, 185–190, 1988.

Saleeby, J. B., Polygenetic ophiolite belt of the California Sierra Nevada: Geochronological and tectonostratigraphic development, *J. Geophys. Res., 87*, 1803–1824, 1982.

Simpson, C., and S. M. Schmid, An evaluation of criteria to deduce the sense of movement in sheared rocks, *Geol. Soc. Am. Bull., 94*, 1281–1288, 1983.

Smithson, S. B., J. A. Brewer, S. Kaufman, J. E. Oliver, and C. A. Hurich, Structure of the Wind River uplift, Wyoming, from COCORP deep reflection data and gravity data, *J. Geophys. Res., 84*, 5955–5972, 1979.

Sonder, L. J., P. C. England, B. P. Wernicke, and R. L. Christiansen, A physical model for Cenozoic extension of western North America, *Spec. Publ. Geol. Soc. London, 28*, 187–201, 1987.

Spry, A., *Metamorphic textures*, 352 pp., Pergamon, New York, 1969.

Stacey, J. S., and J. D. Kramers, Approximation of terrestrial lead isotope evolution by a two-stage model, *Earth Planet. Sci. Lett., 26*, 207–221, 1975.

Tipper, H. W., Mesozoic and Cenozoic geology of the northeastern part of the Mount Waddington map-area (92N), Coast District, British Columbia, *Geol. Surv. Can., Pap. 68-33*, 103 pp., 1969a.

Tipper, H. W., Anahim Lake map-area (93C), *Map 1202A*, Geol. Surv. of Can., Ottawa, Ont., 1969b.

Tipper, H. W., Taseko Lakes map-area (92O), *Open File Map 534*, Geol. Surv. of Can., Ottawa, Ont., 1978.

Tipper, H. W., G. J. Woodsworth, and H. Gabrielse, Tectonic assemblage map of the Canadian Cordillera and adjacent parts of the United States of America, *Map 1505A*, Geol. Surv. of Can., Ottawa, Ont., 1981.

Turner, F. J., and J. Verhoogen, *Igneous and Metamorphic Petrology*, 2nd ed., 694 pp., McGraw-Hill, New York, 1960.

van der Heyden, P., Tectonic and stratigraphic relations between the Coast Plutonic Complex and Intermontane Belt, west-central British Columbia, M.Sc. thesis, 172 pp., Univ. of British Columbia, Vancouver, 1982.

Wenk, E., and F. Keller, Isograde in Amphibolitserien der Zentralalapen, *Schweiz. Mineral. Petrogr. Mitt., 49*, 157–198, 1969.

Wheeler, J. O., and P. McFeely, Tectonic assemblage map of the Canadian Cordillera and adjacent parts of the United States of America, *Open File Map 1565*, Geol. Surv. of Can., Ottawa, Ont., 1987.

White, W. H., G. P. Erickson, K. E. Northcote, G. E. Dirom, and J. E. Harakal, Isotopic dating of the Guichon Batholith, British Columbia, *Can. J. Earth Sci., 4*, 677–690, 1967.

Winkler, H. G. F., *Petrogensis of Metamorphic Rocks*, 334 pp., Springer-Verlag, New York, 1976.

Wust, S. L., Regional correlation of extension directions in Cordilleran metamorphic core complexes, *Geology, 14*, 828–830, 1986.

Yorath, C. J., A. G. Green, R. M. Clowes, A. Sutherland Brown, M. T. Brandon, E. R. Kanasewich, R. D. Hyndman, and C. Spencer, Lithoprobe, southern Vancouver Island: Seismic reflection sees through Wrangellia to the Juan de Fuca plate, *Geology, 13*, 759–762, 1985.

R. L. Armstrong and R. M. Friedman, Department of Geological Sciences, University of British Columbia, Vancouver, B. C., Canada, V6T 2B4.

(Received February 23, 1987;
revised June 21, 1988;
accepted July 8, 1988.)